

Dimensional synthesis of spatial manipulators for velocity and force transmission for operation around a specified task point

Akkarapakam Suneesh Jacob^{1,*} and Bhaskar Dasgupta^{1,+}

¹Affiliation: Indian Institute of Technology Kanpur, Kanpur, India

*Emails: sunjac@iitk.ac.in, suneeshjacob@gmail.com

+Email: dasgupta@iitk.ac.in

ABSTRACT

Dimensional synthesis refers to design of the dimensions of manipulators by optimising different kinds of performance indices. The motivation of this study is to perform dimensional synthesis for a wide set of spatial manipulators by optimising the manipulability of each manipulator around a pre-defined task point in the workspace and to finally give a prescription of manipulators along with their dimensions optimised for velocity and force transmission. A systematic method to formulate Jacobian matrix of a manipulator is presented. Optimisation of manipulability is performed for manipulation of the end-effector around a chosen task point for 96 1-DOF manipulators, 645 2-DOF manipulators, 8 3-DOF manipulators and 15 4-DOF manipulators taken from the result of enumeration of manipulators that is done in its companion paper devoted to enumeration of possible manipulators up to a number of links. Prescriptions for these sets of manipulators are presented along with their scaled condition numbers and their ordered indices. This gives the designer a prescription of manipulators with their optimised dimensions that reflects the performance of the end-effector around the given task point for velocity and force transmission.

Keywords: dimensional synthesis, manipulability, condition number, jacobian, optimisation

1 Introduction

In the context of this study, a manipulator is defined as an assembly of kinematic links connected through kinematic joints, with a fixed base link and a moving end-effector link, in which the end-effector link's motion and force-transformation are controlled by actuating one or more kinematic joints. A kinematic link is a rigid link that can transfer motion and forces, and a kinematic joint is a connection between two links that allows relative motion between the two links. Dimensional synthesis of a manipulator is the problem of designing an appropriate set of dimensions for the manipulator of defined topology¹ to achieve a requirement. Dimensional synthesis problems are generally solved by taking one or more objectives into consideration, such as energy optimisation and well-conditioning of the end-effector's motion. This study focuses on the objective of well-conditioning for velocity and force transmission around a given task point. Well-conditioning is a measure of being distant from singularity. Singularity is related to the local degeneracy of input-output motion/force transformation. A manipulator is said to have a singularity at a point in the joint space if at that configuration the end-effector of the manipulator is unable to be controlled by the actuating joint velocities at least in one direction, either in translation or by rotation. The singularity of a manipulator is often analysed using its Jacobian, the transformation matrix of the joint velocities to the velocity of the end-effector. Using the principle of virtual work, it can be shown that for a system with neg-

ligible frictional power losses the force transmission matrix is exactly the transpose of the velocity transmission matrix. This gives an advantage in designing the dimensions of the manipulators for both inverse force transformation and direct velocity transformation by using the same matrix. Hence, this matrix is used to analyse the singularities of the manipulator. The task of dimensional synthesis is to design the dimensional parameters of various manipulators with the criterion of the maximum extent of singularity avoidance when a representative point in the workspace about which the manipulator's end-effector operates is given along with the bounds of the environment. The criterion used in this study is the manipulability index. The manipulability index for a manipulator would typically be a function of dimensional parameters as variables. The manipulability index with ellipsoidal approach [1] is as follows.

$$\mu = \begin{cases} \sqrt{\det([J][J]^T)} & \text{if } n_j > n_t \\ \sqrt{\det([J]^T[J])} & \text{if } n_j \leq n_t \end{cases} \quad (1)$$

where n_j is the dimension of the joint space and n_t is the dimension of the task space of the manipulator.

The values of the dimensional parameters that would maximise this function would describe the dimensions of the manipulator that would give good performance around the given end-effector point. This concept with ellipsoidal approach is illustrated below for a simple case of a Jacobian matrix that maps linear velocities alone of a 2R-serial planar manipulator.

For a two-link serial manipulator of link lengths l_1 and l_2

¹A specific set of connections of links with specific types of joints

and relative joint angles θ_1 and θ_2 as shown in figure 1, the Jacobian matrix for mapping the linear velocities alone, is given by

$$\begin{Bmatrix} v_x \\ v_y \end{Bmatrix} = \begin{bmatrix} -l_1 \sin \theta_1 - l_2 \sin (\theta_1 + \theta_2) & -l_2 \sin (\theta_1 + \theta_2) \\ l_1 \cos \theta_1 + l_2 \cos (\theta_1 + \theta_2) & +l_2 \cos (\theta_1 + \theta_2) \end{bmatrix} \begin{Bmatrix} \dot{\theta}_1 \\ \dot{\theta}_2 \end{Bmatrix}$$

$$\Rightarrow v_e = [J] \{ \dot{\theta} \}$$

Since the Jacobian matrix in this case is a square matrix, $\sqrt{\det([J]^T[J])} = \det([J])$. The determinant of Jacobian (of transformation of linear velocities) would be

$$\det([J]) = \begin{vmatrix} -l_1 \sin \theta_1 - l_2 \sin (\theta_1 + \theta_2) & -l_2 \sin (\theta_1 + \theta_2) \\ l_1 \cos \theta_1 + l_2 \cos (\theta_1 + \theta_2) & +l_2 \cos (\theta_1 + \theta_2) \end{vmatrix}$$

$$\Rightarrow \det([J]) = l_1 l_2 \sin \theta_2$$

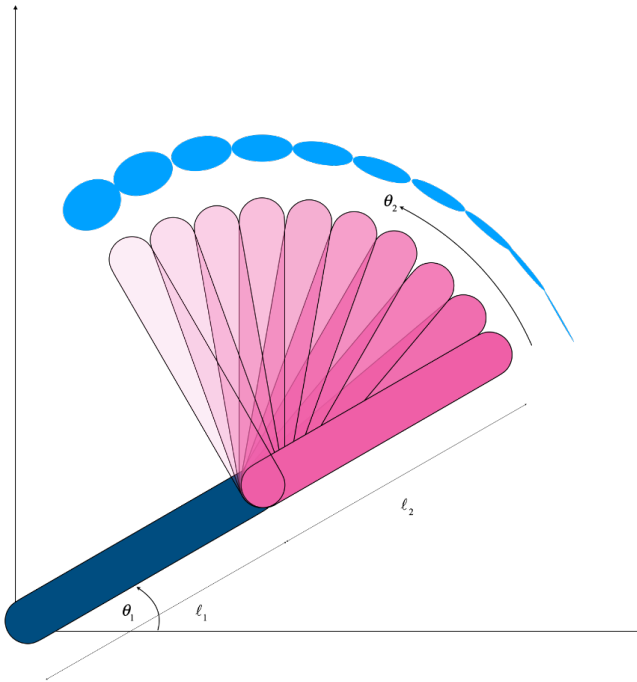


Figure 1. Manipulability varying with θ_2 .

For the determinant to be maximum, the term $l_1 l_2 \sin \theta_2$ needs to be maximum. Since l_1 and l_2 are independent of θ_2 , by assuming them to be constant, $\theta_2 = 90^\circ$ gives the maximum contribution of manipulability independent of l_1 and l_2 , as shown in the figure 1. And by assuming l_1 and l_2 to be varying, $l_1 = l_2$ gives its maximum contribution, as shown in the figure 2. Hence, for a given location of the end-effector, the values θ_1 , θ_2 , l_1 and l_2 can be found.

In the current study, the manipulability index for a specified end-effector point is maximised for various manipulators, and prescriptions are presented for manipulators for same kind of task around the specified point. The same kind of task is reflected by the DOF, and hence the prescriptions of manipulators for each DOF are provided.

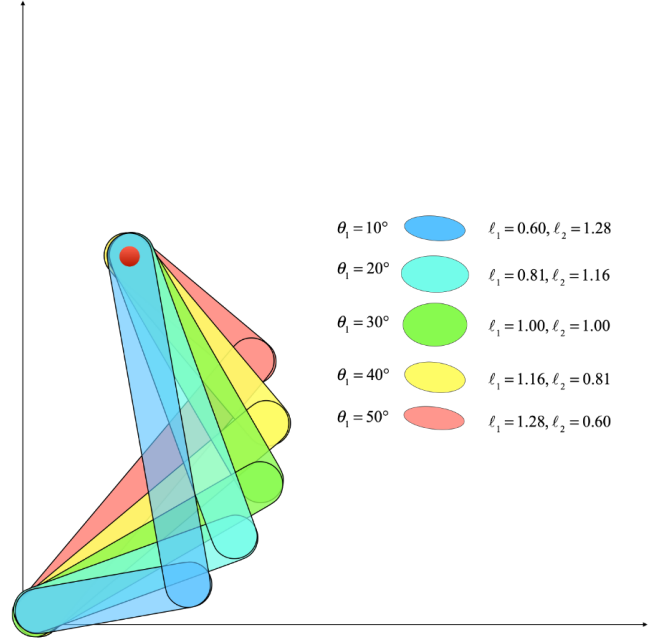


Figure 2. Manipulability varying with l_1 and l_2 .

2 Literature review

Manipulability of a manipulator is calculated by using its Jacobian. In the context of robotics, Jacobian is the matrix that maps the joint-space velocities to the task-space velocities. There are several methods to formulate Jacobian available in the literature. In serial manipulators, only two types of joints, namely prismatic and revolute, are actuated. A standard method to formulate Jacobian for serial manipulators can be found in many books. However, for parallel manipulators, Jacobian formulation becomes more complicated, as the manipulator can contain other types of joints, such as prismatic and spherical joints and can contain passive revolute and prismatic joints. Kevin et al. [2] formulated Jacobian for a novel 6-DOF parallel manipulator by splitting the mapping into two parts, one being the mapping between the end-effector forces/torques and the forces at the spherical joints, and the other being the mapping between the forces at the spherical joints and the torques at the actuating joints. Kim et al. [3] presented a formulation for obtaining analytic Jacobian of parallel manipulators using screw theory. Kim et al. [4] presented the formulation of a new dimensionally homogeneous Jacobian matrix by taking three end-effector points. In their paper, the formulation of Jacobian is done by taking three points of the end-effector platform to interpolate any random point on the platform and differentiating it with respect to time, and finally rewriting the passive joint velocities in terms of active joint velocities and establishing the Jacobian. Geoffrey et al. [5] also formulated a dimensionally homogeneous Jacobian matrix of parallel manipulators for dexterity analysis by using three points on the end-effector platform with a better physical significance of the properties of Jacobian. Liu

et al. [6] presented a method to systematically formulate the dimensionally homogeneous Jacobian when the manipulator has just one type of actuator, i.e., either prismatic or revolute. Their paper shows steps to formulate the generalised Jacobian by using the notation of screw theory. Hu [7] presented a formulation of unified Jacobian for serial-parallel manipulators, i.e., a set of parallel manipulators linked one upon the other, serially. Even though there are many systematic formulations of Jacobian in the literature, there appears to be no unique method of systematic formulation of Jacobian that is applicable for both serial and parallel manipulators (including closed-loop spatial kinematic chains). In this study, a systematic formulation of Jacobian is presented that is applicable for both serial and parallel manipulators (including closed-loop spatial kinematic chains) containing four types of joints, namely revolute, prismatic, cylindrical and spherical.

Condition number of Jacobian is the ratio of maximum and minimum singular values of the Jacobian. It gives a measure of how much the manipulability is distributed to each singular value. Sometimes the manipulability measure alone might be unable to capture the information about singularity at a configuration in which case the condition number could give more information. For example, if a Jacobian has three singular values 100000, 0.00002 and 3, the singular value 0.00002 shows that it is close to singularity. But the manipulability would be 6, from which it is not very clear that it is close to singularity, whilst the condition number would be 5×10^9 which indicates that the manipulability is not equally distributed. Hence, condition numbers at the optimal configurations of the manipulators are important to analyse the performances. Jacobian is a mapping from joint velocities to end-effector velocities. This includes both the linear and the angular velocities of the end-effector that have different units. Similarly, the transpose of Jacobian maps the joint torques/forces to both forces and moments of the end-effector, which again have different units. This difference in units makes it difficult to assess the significance of the condition number of Jacobian. It is discussed in the literature that due to the non-uniform dimensions of the elements of the Jacobian matrix, the condition number may have little physical significance. Doty et al. [8] identified the problem of difference in units of elements of Jacobian and the difficulties associated with it. Angeles [9] used the concept of natural length to present the Jacobian matrix in dimensionless form. In his paper, the natural length is chosen such that the condition number of the Jacobian matrix is minimised. Stocco et al. [10] used a scaling matrix with which the Jacobian matrix is to be multiplied in order to normalise the units of the Jacobian matrix and to use it with a performance goal. Their paper chooses the scaling matrix based on maximum desired forces. Ma et al. [11] discussed non-uniformity of units in the elements of Jacobian matrix, and used characteristic length to homogenise the Jacobian matrix. In their paper, a homogenised form of Jacobian matrix is presented for a 6-DOF platform manipulator, with characteristic length as a chosen parameter. In their paper,

they suggested a scaling of the Jacobian matrix by multiply-

ing it with the matrix $[S] = \begin{bmatrix} \frac{1}{L} & 0 & 0 & 0 & 0 & 0 \\ 0 & \frac{1}{L} & 0 & 0 & 0 & 0 \\ 0 & 0 & \frac{1}{L} & 0 & 0 & 0 \\ 0 & 0 & 0 & 1 & 0 & 0 \\ 0 & 0 & 0 & 0 & 1 & 0 \\ 0 & 0 & 0 & 0 & 0 & 1 \end{bmatrix}$ where

L is called the characteristic length. As mentioned in their paper, there are many ways to define the characteristic length depending on the interest of the user. Various proposals of characteristic length were made in the literature, depending on the orientation of the problem that is to be solved. Their paper chose L , for platform manipulators of spherical joints, as the average of the distances from the centroid of the moving plate to each of the joints.

Yoshikawa [1] used the concept of singular values of Jacobian matrix as the manipulability measure to describe the performance of manipulators. Lee [12] used the concept of manipulability polytypes as a competing measure of manipulability. In his paper, the manipulability measure through manipulability ellipsoids is compared with that of manipulability polytopes. The paper concludes that the polytope approach can represent the manipulability more accurately than that of the ellipsoid approach, as the ellipsoid would not be covering the entire region of the set of unit joint velocities in the joint-space. Even though the polytope approach represents a better description of manipulability measure than the ellipsoid approach, the ellipsoid approach is simple to implement. To reduce the computational complexity and for simplicity, the ellipsoid approach is implemented in this study.

Khezrian et al. [13], in their paper, designed a spherical 3-DoF parallel manipulator by maximising Global Dynamic Conditioning Index. In their paper, the Global Dynamic Conditioning Index of the manipulator is optimised, and the optimal dimensional parameters are presented. Hazarathiah [14] presented a prescription of several planar manipulators of revolute joints with corresponding optimised manipulability indices and condition numbers for a specified task position. In his thesis, several planar manipulators are presented, and the manipulability index of each manipulator is calculated as a function of its dimensional parameters. For each of the manipulators, the manipulability index is maximised, and the corresponding dimensions are presented. But this is limited to planar manipulators with revolute type of joints. The current study presents the prescriptions for several spatial manipulators with four types of joints, namely revolute, prismatic, cylindrical and spherical joints.

3 Methodology

3.1 Methodology to formulate Jacobian

The method used to generate Jacobian matrices for the manipulators in the context of this study is based on identifying all possible connecting paths from the base link to the end-effector link and kinematically formulating linear and angular velocities of the end-effector link through these paths, and

finally transforming the passive joint velocities in terms of active joint velocities.

Identifying all possible connecting paths:

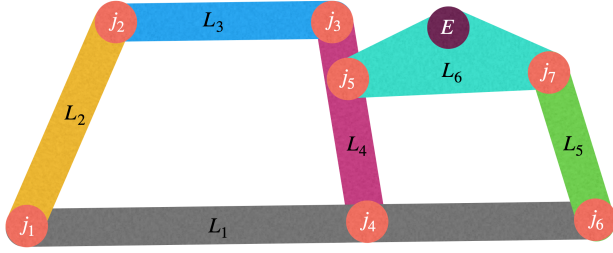


Figure 3. A mechanism with loops for illustration.

For the manipulator depicted in figure 3, the connecting paths from the base link to the end-effector link are shown below.

Path 1: $L_1 - j_1 - L_2 - j_2 - L_3 - j_3 - L_4 - j_5 - L_6$

Path 2: $L_1 - j_4 - L_4 - j_5 - L_6$

Path 3: $L_1 - j_6 - L_5 - j_7 - L_6$

Formulating linear and angular velocities:

Each consecutive pair of links of the connecting path is considered to cumulatively formulate linear and angular velocities from the base link to the end-effector link, as each joint contributes linear and angular velocities to the end-effector link. For each consecutive pair of links in the connecting path, the contributions to the angular velocity and the linear velocity of the end-effector are given by $\vec{\omega}_{ij}$ and \vec{v}_{ij} respectively in various cases, as shown in table 1.

Joint type	$\vec{\omega}_{ij}$	\vec{v}_{ij}
Revolute	$\dot{\theta}_{ij}\hat{n}_{ij}$	$\dot{\theta}_{ij}\hat{n}_{ij} \times (\vec{a} - \vec{r}_{ij})$
Prismatic	0	$\dot{d}_{ij}\hat{n}_{ij}$
Cylindrical	$\dot{\theta}_{ij}\hat{n}_{ij}$	$\dot{\theta}_{ij}\hat{n}_{ij} \times (\vec{a} - \vec{r}_{ij}) + \dot{d}_{ij}\hat{n}_{ij}$
Spherical	$\vec{\omega}_{ij}$	$\vec{\omega}_{ij} \times (\vec{a} - \vec{r}_{ij})$

Table 1. Result of the optimisation problem corresponding to 2D-M71 manipulator.

And the angular and linear velocities of the end-effector, described through the connecting path, are given by the sum of all the components of angular velocities and the sum of all the components of linear velocities contributed to the end-effector, respectively. Here, $\vec{r}_{ij} = \{r_{ijx} \ r_{ijy} \ r_{ijz}\}^T$ and $\hat{n}_{ij} = \{n_{ijx} \ n_{ijy} \ n_{ijz}\}^T$ represent the position vector of the instantaneous location and the axis of the instantaneous motion respectively, of the joint connected to the links L_i & L_j , and $\vec{\omega}_{ij} = \{\omega_{ijx} \ \omega_{ijy} \ \omega_{ijz}\}^T$ represents the relative angular velocity vector of the link L_j relative to the link L_i , of the adjacency matrix. $\vec{a} = \{a_x \ a_y \ a_z\}^T$ is the position vector of the end-effector, and $\dot{\theta}_{ij}$ and \dot{d}_{ij} represent the translational and the rotational joint velocities respectively, of the joint

connected to the links L_i and L_j of the adjacency matrix, measured relative to the link L_i .

Applying the above process to each connecting path from base link to end-effector link gives the description of velocity of the end-effector in terms of linear combinations of active and passive joint velocities, the coefficients being functions of the configuration parameters of the manipulator, i.e., r_{ijx} , r_{ijy} , r_{ijz} , β_{ij} , ϕ_{ij} , a_x , a_y and a_z , where $\vec{a} = \{a_x \ a_y \ a_z\}^T$ is the position vector of the end-effector point. For the particular kind of manipulator shown in figure 3, there are three paths and hence three descriptions of pairs of angular and linear velocities can be formulated as $\begin{Bmatrix} v_1 \\ \omega_1 \end{Bmatrix}$, $\begin{Bmatrix} v_2 \\ \omega_2 \end{Bmatrix}$ and $\begin{Bmatrix} v_3 \\ \omega_3 \end{Bmatrix}$, each expressed in the form of linear combinations of active and passive velocities as shown in equation (2) for all i .

$$\begin{Bmatrix} v^{(i)} \\ \omega^{(i)} \end{Bmatrix} = [J^{(i)}] \begin{Bmatrix} \dot{\theta}_a \\ \Omega \end{Bmatrix} = [J_1^{(i)}] \begin{Bmatrix} \dot{\theta}_a \end{Bmatrix} + [J_2^{(i)}] \begin{Bmatrix} \Omega \end{Bmatrix} \quad (2)$$

Each of $\begin{Bmatrix} v^{(i)} \\ \omega^{(i)} \end{Bmatrix}$ would represent the velocity components of the end-effector. Since the Jacobian matrix is a mapping of end-effector velocities with active joint velocities, all the passive joint velocities, i.e., all the variables $\dot{\theta}_{ij}$, \dot{d}_{ij} , ω_{ijx} , ω_{ijy} and ω_{ijz} other than the actuating joint velocities, are to be written in terms of active joint velocities. The number of independent formulations of velocities (through the identified connecting paths from the base link to the end-effector link) should be more than or equal to the number of passive joint velocities that are to be eliminated. Once the passive joint velocities are written in terms of linear combinations of actuating joint velocities, the velocities of the end-effector can be expressed as a mapping of actuating joint velocities alone, and the mapping matrix thus generated would be the Jacobian matrix. The convention followed in this study in order to formulate the Jacobian matrix is to consider $\begin{Bmatrix} v_1 \\ \omega_1 \end{Bmatrix}$ as the pair of linear and angular velocities of the end-effector as shown in equation (3) and to consider $\begin{Bmatrix} v_i - v_1 \\ \omega_i - \omega_1 \end{Bmatrix}$ for all $i \neq 1$ to form the matrices $[A_1]$ and $[A_2]$, as shown in equation (4), where N is the number of paths from base link to end-effector link of the manipulator.

$$\begin{Bmatrix} v \\ \omega \end{Bmatrix} = \begin{Bmatrix} v_1 \\ \omega_1 \end{Bmatrix} = [J_1] \begin{Bmatrix} \dot{\theta}_a \end{Bmatrix} + [J_2] \begin{Bmatrix} \Omega \end{Bmatrix} \quad (3)$$

$$\begin{Bmatrix} v_2 - v_1 \\ v_3 - v_1 \\ \dots \\ v_N - v_1 \\ \omega_2 - \omega_1 \\ \omega_3 - \omega_1 \\ \dots \\ \omega_N - \omega_1 \end{Bmatrix} = [A] \begin{Bmatrix} \dot{\theta} \end{Bmatrix} = [A_1] \begin{Bmatrix} \dot{\theta}_a \end{Bmatrix} + [A_2] \begin{Bmatrix} \Omega \end{Bmatrix} = 0 \quad (4)$$

From (4), if A_2 is invertible, the passive joint velocities can be written in terms of active joint velocities as shown in (5).

$$\{\Omega\} = -[A_2]^{-1}[A_1]\{\dot{\theta}_a\} \quad (5)$$

By putting (5) in (3), the pair of linear and angular velocities of the end-effector can be written in terms of active joint velocities alone, as shown in (6).

$$\begin{aligned} \begin{Bmatrix} v \\ \omega \end{Bmatrix} &= [J_1]\{\dot{\theta}_a\} - [J_2][A_2]^{-1}[A_1]\{\dot{\theta}_a\} \\ &= \left([J_1] - [J_2][A_2]^{-1}[A_1]\right)\{\dot{\theta}_a\} \\ &= [\tilde{J}]\{\dot{\theta}_a\} \end{aligned} \quad (6)$$

From equation (6), Jacobian of the manipulator can be defined as $[\tilde{J}] = [J_1] - [J_2][A_2]^{-1}[A_1]$ and the elements of Jacobian would be functions of configuration parameters, i.e., $r_{ijx}, r_{ijy}, r_{ijz}, n_{ijx}, n_{ijy}, n_{ijz}, a_x, a_y$ and a_z .

3.1.1 The case of superfluous DOF

If the system of equations $[A]\{\dot{\theta}\} = 0$ happens to have less equations than the number of unknowns then it signifies that the equations are inadequate to determine all the unknowns. Assuming that the right number of DOF is considered in the formulation, this could happen when the mechanism has a superfluous DOF. Superfluous DOF, in the context of this study, is the part of DOF of the mechanism that is not needed to impart the end-effector link to desired motion, which is the rotation of a link or a set of connected links of a mechanism, about an axis passing through the centres of two spherical joints, which does not alter either linear velocity or angular velocity of the end-effector. An example of superfluous DOF is the rotation of the link connected by two spherical joints about an axis that passes through the centres of the two spherical joints in the four-bar RSSR spatial manipulator, as shown in figure 4.

An appropriate fix is made in this study that can enable the calculation of manipulability index. In the first step, the link (or the set of links) connected to the rest of the mechanism by two spherical joints alone, is identified. The angular velocity of the link (or the set of links) about the axis passing through the two spherical joints is to be set to zero. This can be achieved by the equation (7), where $\vec{\omega}_k$ is the absolute velocity of the link if it is the case of a single link (and is the absolute velocity of any link that is connected to one of the spherical joints if it is the case of a set of links), \vec{r}_{ij} and \vec{r}_{kl} are the position vectors of the two spherical joints.

$$\vec{\omega}_k \cdot (\vec{r}_{ij} - \vec{r}_{kl}) = 0 \quad (7)$$

This fixes the issue and enables to calculate the manipulability index. Here, the superfluous angular velocity of the link is set to zero for simplicity, although setting it to any other value also fixes the issue.

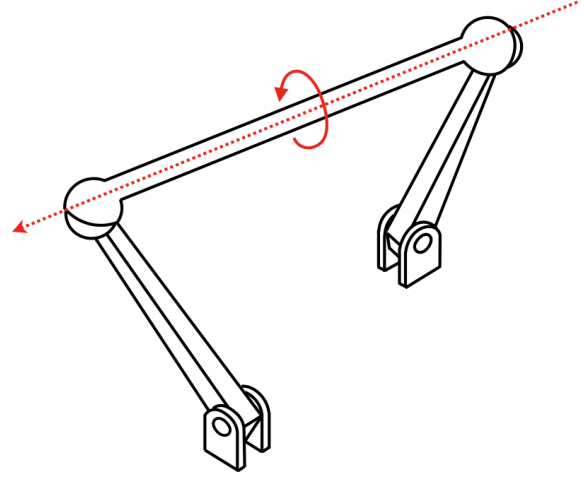


Figure 4. RSSR mechanism as an example of superfluous DOF.

3.1.2 Type-2 singularity

The formulation of Jacobian given by the equation (6) can be calculated only if $[A_2]$ is invertible. If it is not invertible, then the calculation of Jacobian would break down. Furthermore, any configuration close to such a configuration would end up having its Jacobian potentially badly scaled due to their singular values being close to zero. This is a type of singularity [15] widely known as Type-2 singularity [16, 17, 18, 19, 20, 21], and this exists only in parallel manipulators (including closed-loop kinematic manipulators of single DOF, etc.), as $[A_2]$ does not come into picture in case of serial manipulators.

3.2 Methodology to formulate condition number of a scaled matrix

Since revolute, prismatic, cylindrical and spherical joints are used in the current study, the characteristic length used in this study is defined as follows.

If all the joints of a given manipulator are prismatic, then scaling is not needed. Suppose the manipulator consists of revolute joints or cylindrical joints. In that case, an effective distance is considered for each joint, which is the shortest distance between the end-effector point and the axis of rotation of the revolute joint. If the position vector of the joint is \vec{r}_{ij} and the end-effector point is \vec{a} and the unit vector along the axis of the rotation is \hat{n}_{ij} then the effective distance is given by $\vec{d} = |(\vec{r}_{ij} - \vec{a}) \times \hat{n}_{ij}|$. If there are spherical joints in the manipulator, then in such case, the effective distance for each spherical joint is the distance between the end-effector point and the centre of the spherical joint. If the position vector of the joint is \vec{r}_{ij} and the end-effector point is \vec{a} then the effective distance is given by $\vec{d} = |\vec{r}_{ij} - \vec{a}|$. And finally, the characteristic length L is calculated as the average of all these effective distances. Once the characteristic length is calculated, the scaling matrix $[S]$ can be formed and multiplied

appropriately to the actual Jacobian matrix to get the scaled Jacobian matrix ($[J_S] = [S][J]$). And the condition number for this scaled Jacobian matrix $[J_S]$ is used for comparison of manipulators in this study.

The manipulators are sorted by their corresponding condition numbers in ascending order, and the corresponding indices are presented in the 2-DOF, 3-DOF and 4-DOF prescriptions by the name i_k .

3.3 Methodology to formulate optimisation problem

In the current study, dimensional synthesis of all the enumerated manipulators is performed for the task position represented by the position vector of the end-effector point, which is arbitrarily chosen in this study as $\vec{a} = 3\hat{i} + 4\hat{j} + 5\hat{k}$. This task position is used for all the manipulators here, for which dimensional synthesis is done. All the dimensions of manipulators in this study are in S.I. units.

The objective function is the manipulability index which is given by equation 1.

The manipulators used in the current study have four types of joints: revolute, prismatic, cylindrical and spherical. When the applicable positions and orientations of the joints are defined, the dimensions of the manipulator can be determined. Thus, the objective function would be a function of the applicable positions and orientations of the joints.

The elements of Jacobian matrix would be functions of configuration parameters, i.e., r_{ijx} , r_{ijy} , r_{ijz} , n_{ijx} , n_{ijy} and n_{ijz} . The manipulability measure of the manipulator is the product of singular values, which would be a scalar function of the configuration parameters. It can be calculated by the expression $\mu = \sqrt{\det([J]^T[J])}$ if the number of actuating joints is less than or equal to the number of independent scalar quantities of the output velocity and $\mu = \sqrt{\det([J][J]^T)}$ otherwise. In the context of the current study, the spatial manipulators have up to six degrees of freedom. Since the enumerated list of manipulators in this study comprises 1-DOF, 2-DOF, 3-DOF, and 4-DOF manipulators, the number of actuating joints would be at most 4, which is less than 6. And hence $\mu = \sqrt{\det([J]^T[J])}$ is considered for all the manipulators.

For simplicity in calculations, it is assumed that the locations of the joints should be within the cube of length 10m in the first octave with one of its corners at origin. Therefore the optimisation problem for each of the manipulators can be defined as follows.

Maximise

$$\mu = \sqrt{\det([J]^T[J])}$$

subject to constraints

$$n_{ijx}^2 + n_{ijy}^2 + n_{ijz}^2 = 1,$$

$$0 \leq r_{ijx} \leq 10,$$

$$0 \leq r_{ijy} \leq 10,$$

$$0 \leq r_{ijz} \leq 10.$$

In parallel manipulators, two new types of singularities arise, making the total number of types of singularities to be three. A normal mapping of end-effector velocities and joint velocities for parallel manipulators is typically expressed in the form as shown in equation (8).

$$\{\dot{X}\} = \left([J_1] - [J_2][A_2]^{-1}[A_1] \right) \{\dot{\theta}\} \quad (8)$$

If $[A_2]$ is singular then the product of singular values of Jacobian would become infinity. The physical significance of this is that at a particular set of dimensions the end-effector gains a DOF that cannot be controlled by the joint velocities. Equation (8) can be written in a more simplified form as

$$\begin{aligned} \det([A_2])[I]\{\dot{X}\} + ([J_2] \text{adj}([A_2])[A_1] - \det([A_2])[J_1])\{\dot{\theta}\} &= 0 \\ \Rightarrow [\tilde{A}]\{\dot{X}\} + [\tilde{B}]\{\dot{\theta}\} &= 0 \end{aligned}$$

where $[\tilde{A}] = \det([A_2])[I]$ and $[\tilde{B}] = [J_2] \text{adj}([A_2])[A_1] - \det([A_2])[J_1]$.

The three types [22] of singularities are outlined below.

Type 1 singularity: When the product of singular values of $[\tilde{B}]$ is zero, it is referred to as type 1 singularity, which is commonly encountered in serial manipulators and also parallel manipulators.

Type 2 singularity: When the product of singular values of $[\tilde{A}]$ is zero, it is referred to as type 2 singularity, which is encountered only in parallel manipulators.

Type 3 singularity: When both the products of singular values of $[\tilde{A}]$ and $[\tilde{B}]$ are individually zero, it is referred to as type 3 singularity.

These are compactly summarised in table 2.

Singularity type	Condition
Type 1	$[\tilde{B}]$ is singular
Type 2	$[\tilde{A}]$ is singular
Type 3	Both $[\tilde{A}]$ and $[\tilde{B}]$ are singular

Table 2. Various types of singularities.

Since a zero singular value of either of the matrices could lead to singularity, in order to design for optimal performance, the function $f_2 = \sqrt{\det([\tilde{A}]^T[\tilde{A}]) \det([\tilde{B}]^T[\tilde{B}])}$ is used [14] in optimisation whenever $f_1 = \sqrt{\det([\tilde{J}]^T[\tilde{J}])}$ of the manipulator becomes infinity during optimisation process.

3.4 Strategy used in the optimisation process

Since classical optimisation algorithms can find only local minima, multiple initial guesses are considered to reasonably attempt to find global optima. The following strategy is used with consideration of identifying and handling the cases involving type 2 and type 3 singularities.

For each manipulator, the following four steps are performed.

Step 1: Maximisation of $f_1 = \sqrt{\det([J]^T [J])}$ with 100 random initial guesses within the bounds. The local optimal points for which the condition number of $[\tilde{A}]$ is less than 1000 and the minimum singular value of $[\tilde{A}]$ is greater than 10^{-2} , are shortlisted. For serial manipulators $[\tilde{A}]$ does not exist and hence this step is omitted for serial manipulators.

Step 2: The maximum of these shortlisted points is considered to be the optimal point.

Step 3: If no point passes the shortlisting criteria, then it is assumed that type 2 or type 3 singularity has occurred. And

hence, maximisation of $f_2 = \sqrt{\det([\tilde{A}]^T [\tilde{A}]) \det([\tilde{B}]^T [\tilde{B}])}$ is performed with a random initial guess.

Step 4: In step 3, for the local optimum point, if the condition number of Jacobian is less than 1000 and the minimum singular value of Jacobian is greater than 10^{-2} , then the point is considered as the optimal point. If the condition number is greater than or equal to 1000 or if the minimum singular value is less than or equal to 10^{-2} or if the initial guess does not converge, then this initial guess is discarded, and a new random initial guess is used to repeat step 3 until the initial guess converges, the condition number ends up to be less than 1000, and the minimum singular value ends up to be greater than 10^{-2} .

The built-in command *fmincon* of MATLAB Optimisation Toolbox [23], with default options, is used to perform optimisation in this study. The default method that the command uses for this kind of optimisation problems is *interior-point* with BFGS approximation of Hessian. The interior-point method is used to handle constrained optimisation, which uses a barrier function that pressurises the point during the iterations to lie within the boundary of the feasible space.

Some parameters used by the MATLAB function are

- Constraint Tolerance: 10^{-6}
- Finite Difference Type: Forward
- Function Tolerance: 10^{-6}
- Step Tolerance: 10^{-10}

4 Dimensional synthesis

From a previous companion study [24] on the enumeration of manipulators, 96 1-DOF manipulators amongst 4 links and 645 2-DOF, 8 3-DOF and 15 4-DOF manipulators amongst 3, 4 and 5 links are considered for dimensional synthesis. All joints are actuated in case of serial manipulators, whereas

there exist passive joints in case of closed-loop manipulators. Appropriate actuating joints are arbitrarily chosen from revolute and prismatic joints of the closed-loop manipulators. Dimensional synthesis for all the manipulators is performed based on the methodology presented in section 3.

As an example, detailed steps for dimensional synthesis of the manipulator 2D-M71 is shown below.

4.1 Detailed formulation of the manipulator 2D-M71 as an example

The schematic diagram of 2D-M71 manipulator is shown in figure 5, mentioning the actuator joints in cyan circles.

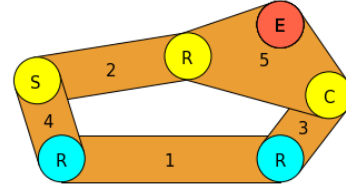


Figure 5. Schematic figure of 2D-M71.

Formulation of Jacobian:

Jacobian of the manipulator is formulated using the steps shown in section 3.1. The various paths that connect the base link and the end-effector link are $L_1 - R - L_3 - C - L_5$ and $L_1 - R - L_4 - S - L_2 - R - L_5$. The descriptions of linear and angular velocities of the end-effector is formulated using various paths from the end-effector link to the base link, and shown by the equations below.

$$\vec{v} = \dot{\theta}_{13} \hat{n}_{13} \times (\vec{a} - \vec{r}_{13}) + \dot{\theta}_{35} \hat{n}_{35} \times (\vec{a} - \vec{r}_{35}) + \dot{d}_{35} \hat{n}_{35} \quad (9)$$

$$\vec{v} = \dot{\theta}_{14} \hat{n}_{14} \times (\vec{a} - \vec{r}_{14}) + \vec{\omega}_{42} \times (\vec{a} - \vec{r}_{42}) + \dot{\theta}_{25} \hat{n}_{25} \times (\vec{a} - \vec{r}_{25}) \quad (10)$$

$$\vec{\omega} = \dot{\theta}_{13} \hat{n}_{13} + \dot{\theta}_{35} \hat{n}_{35} \quad (11)$$

$$\vec{\omega} = \dot{\theta}_{14} \hat{n}_{14} + \vec{\omega}_{42} + \dot{\theta}_{25} \hat{n}_{25} \quad (12)$$

where $\vec{r}_{ij} = \begin{Bmatrix} r_{ijx} \\ r_{ijy} \\ r_{ijz} \end{Bmatrix}$ and $\hat{n}_{ij} = \begin{Bmatrix} n_{ijx} \\ n_{ijy} \\ n_{ijz} \end{Bmatrix}$ represent the position vector of the instantaneous location and the axis of the instantaneous motion respectively, of the joint connected to the links L_i & L_j , and $\vec{\omega}_{ij} = \begin{Bmatrix} \omega_{ijx} \\ \omega_{ijy} \\ \omega_{ijz} \end{Bmatrix}$ represents the relative angular velocity vector of the link L_j relative to the link L_i . $\vec{a} = \begin{Bmatrix} a_x \\ a_y \\ a_z \end{Bmatrix}$ is the position vector of the end-effector, and $\dot{\theta}_{ij}$

and \dot{d}_{ij} represent the translational and the rotational joint velocities respectively, of the joint connected to the links L_i and L_j , measured relative to the link L_i .

From equations (9) and (11), the vector of end-effector velocities in terms of both active and passive joint angles is given by

$$\begin{aligned} \begin{Bmatrix} \vec{v} \\ \vec{\omega} \end{Bmatrix} &= \begin{bmatrix} n_{13y}(a_z - r_{13z}) - n_{13z}(a_y - r_{13y}) & 0 & n_{35x} & 0 \\ -n_{13x}(a_z - r_{13z}) + n_{13z}(a_x - r_{13x}) & 0 & n_{35y} & 0 \\ n_{13x}(a_y - r_{13y}) - n_{13y}(a_x - r_{13x}) & 0 & n_{35z} & 0 \\ n_{13x} & 0 & 0 & 0 \\ n_{13y} & 0 & 0 & 0 \\ n_{13z} & 0 & 0 & 0 \end{bmatrix} \begin{Bmatrix} \dot{\theta}_{13} \\ \dot{\theta}_{14} \\ \dot{d}_{35} \\ \dot{\theta}_{25} \\ \dot{\theta}_{35} \\ \omega_{42x} \\ \omega_{42y} \\ \omega_{42z} \end{Bmatrix} \\ &\Rightarrow \begin{Bmatrix} \vec{v} \\ \vec{\omega} \end{Bmatrix} = \begin{bmatrix} n_{13y}(a_z - r_{13z}) - n_{13z}(a_y - r_{13y}) & 0 \\ -n_{13x}(a_z - r_{13z}) + n_{13z}(a_x - r_{13x}) & 0 \\ n_{13x}(a_y - r_{13y}) - n_{13y}(a_x - r_{13x}) & 0 \\ n_{13x} & 0 \\ n_{13y} & 0 \\ n_{13z} & 0 \end{bmatrix} \begin{Bmatrix} \dot{\theta}_{13} \\ \dot{\theta}_{14} \end{Bmatrix} + \\ &\begin{bmatrix} n_{35x} & 0 & n_{35y}(a_z - r_{35z}) - n_{35z}(a_y - r_{35y}) & 0 & 0 & 0 \\ n_{35y} & 0 & -n_{35x}(a_z - r_{35z}) + n_{35z}(a_x - r_{35x}) & 0 & 0 & 0 \\ n_{35z} & 0 & n_{35x}(a_y - r_{35y}) - n_{35y}(a_x - r_{35x}) & 0 & 0 & 0 \\ 0 & 0 & n_{35x} & 0 & 0 & 0 \\ 0 & 0 & n_{35y} & 0 & 0 & 0 \\ 0 & 0 & n_{35z} & 0 & 0 & 0 \end{bmatrix} \begin{Bmatrix} \dot{d}_{35} \\ \dot{\theta}_{25} \\ \dot{\theta}_{35} \\ \omega_{42x} \\ \omega_{42y} \\ \omega_{42z} \end{Bmatrix} \\ &\Rightarrow \begin{Bmatrix} \vec{v} \\ \vec{\omega} \end{Bmatrix} = [J_1] \{ \dot{\theta}_a \} + [J_2] \{ \Omega \} \end{aligned}$$

where $\{ \dot{\theta}_a \} = \begin{Bmatrix} \dot{\theta}_{13} \\ \dot{\theta}_{14} \end{Bmatrix}$ and $\{ \Omega \} = \begin{Bmatrix} \dot{d}_{35} \\ \dot{\theta}_{25} \\ \dot{\theta}_{35} \\ \omega_{42x} \\ \omega_{42y} \\ \omega_{42z} \end{Bmatrix}$ represent the active joint-velocities and the passive joint-velocities, respectively.

But since the Jacobian should contain the end-effector velocities in terms of active joint angles alone, the passive joint angles must be written in terms of active joint angles. From the two equations (10) and (9),

$$\begin{aligned} \dot{\theta}_{13} \hat{n}_{13} \times (\vec{a} - \vec{r}_{13}) + \dot{\theta}_{35} \hat{n}_{35} \times (\vec{a} - \vec{r}_{35}) \\ + \dot{d}_{35} \hat{n}_{35} = \dot{\theta}_{14} \hat{n}_{14} \times (\vec{a} - \vec{r}_{14}) \\ + \vec{\omega}_{42} \times (\vec{a} - \vec{r}_{42}) + \dot{\theta}_{25} \hat{n}_{25} \times (\vec{a} - \vec{r}_{25}) \end{aligned} \quad (13)$$

From the two equations (12) and (11),

$$\dot{\theta}_{14} \hat{n}_{14} + \vec{\omega}_{42} + \dot{\theta}_{25} \hat{n}_{25} = \dot{\theta}_{13} \hat{n}_{13} + \dot{\theta}_{35} \hat{n}_{35} \quad (14)$$

From the equations (13) and (14), linear equations in terms of active and passive joint angles can be stacked as shown below, using which the passive joint angles can be written in terms of the active joint angles.

$$\begin{bmatrix} -n_{13y}(a_z - r_{13z}) + n_{13z}(a_y - r_{13y}) \\ n_{13x}(a_z - r_{13z}) - n_{13z}(a_x - r_{13x}) \\ -n_{13x}(a_y - r_{13y}) + n_{13y}(a_x - r_{13x}) \\ -n_{13x} \\ -n_{13y} \\ -n_{13z} \\ n_{14y}(a_z - r_{14z}) - n_{14z}(a_y - r_{14y}) \\ -n_{14x}(a_z - r_{14z}) + n_{14z}(a_x - r_{14x}) \\ n_{14x}(a_y - r_{14y}) - n_{14y}(a_x - r_{14x}) \\ n_{14x} \\ n_{14y} \\ n_{14z} \\ -n_{35x} & n_{25y}(a_z - r_{25z}) - n_{25z}(a_y - r_{25y}) \\ -n_{35y} & -n_{25x}(a_z - r_{25z}) + n_{25z}(a_x - r_{25x}) \\ -n_{35z} & n_{25x}(a_y - r_{25y}) - n_{25y}(a_x - r_{25x}) \\ 0 & n_{25x} \\ 0 & n_{25y} \\ 0 & n_{25z} \\ -n_{35y}(a_z - r_{35z}) + n_{35z}(a_y - r_{35y}) & 0 \\ n_{35x}(a_z - r_{35z}) - n_{35z}(a_x - r_{35x}) & -a_z + r_{42z} \\ -n_{35x}(a_y - r_{35y}) + n_{35y}(a_x - r_{35x}) & a_y - r_{42y} \\ -n_{35x} & 1 \\ -n_{35y} & 0 \\ -n_{35z} & 0 \end{bmatrix} \begin{Bmatrix} \dot{\theta}_{13} \\ \dot{\theta}_{14} \\ \dot{d}_{35} \\ \dot{\theta}_{25} \\ \dot{\theta}_{35} \\ \omega_{42x} \\ \omega_{42y} \\ \omega_{42z} \end{Bmatrix} = \begin{Bmatrix} 0 \\ 0 \\ 0 \\ 0 \\ 0 \\ 0 \\ 0 \\ 0 \\ 0 \\ 0 \\ 0 \\ 0 \\ 0 \\ 0 \\ 0 \\ 0 \\ 0 \\ 0 \\ 0 \\ 0 \end{Bmatrix}$$

$$\begin{bmatrix} a_z - r_{42z} & -a_y + r_{42y} \\ 0 & a_x - r_{42x} \\ -a_x + r_{42x} & 0 \\ 0 & 0 \\ 1 & 0 \\ 0 & 1 \end{bmatrix} \begin{Bmatrix} \dot{\theta}_{13} \\ \dot{\theta}_{14} \\ \dot{d}_{35} \\ \dot{\theta}_{25} \\ \dot{\theta}_{35} \\ \omega_{42x} \\ \omega_{42y} \\ \omega_{42z} \end{Bmatrix} = \begin{Bmatrix} 0 \\ 0 \\ 0 \\ 0 \\ 0 \\ 0 \\ 0 \\ 0 \end{Bmatrix}$$

$$\Rightarrow \begin{bmatrix} -n_{13y}(a_z - r_{13z}) + n_{13z}(a_y - r_{13y}) \\ n_{13x}(a_z - r_{13z}) - n_{13z}(a_x - r_{13x}) \\ -n_{13x}(a_y - r_{13y}) + n_{13y}(a_x - r_{13x}) \\ -n_{13x} \\ -n_{13y} \\ -n_{13z} \end{bmatrix}$$

$$\begin{bmatrix} n_{14y}(a_z - r_{14z}) - n_{14z}(a_y - r_{14y}) \\ -n_{14x}(a_z - r_{14z}) + n_{14z}(a_x - r_{14x}) \\ n_{14x}(a_y - r_{14y}) - n_{14y}(a_x - r_{14x}) \\ n_{14x} \\ n_{14y} \\ n_{14z} \end{bmatrix} \begin{Bmatrix} \dot{\theta}_{13} \\ \dot{\theta}_{14} \end{Bmatrix} +$$

$$\begin{bmatrix} -n_{35x} & n_{25y}(a_z - r_{25z}) - n_{25z}(a_y - r_{25y}) \\ -n_{35y} & -n_{25x}(a_z - r_{25z}) + n_{25z}(a_x - r_{25x}) \\ -n_{35z} & n_{25x}(a_y - r_{25y}) - n_{25y}(a_x - r_{25x}) \\ 0 & n_{25x} \\ 0 & n_{25y} \\ 0 & n_{25z} \end{bmatrix}$$

$$\begin{bmatrix} -n_{35y}(a_z - r_{35z}) + n_{35z}(a_y - r_{35y}) & 0 \\ n_{35x}(a_z - r_{35z}) - n_{35z}(a_x - r_{35x}) & -a_z + r_{42z} \\ -n_{35x}(a_y - r_{35y}) + n_{35y}(a_x - r_{35x}) & a_y - r_{42y} \\ -n_{35x} & 1 \\ -n_{35y} & 0 \\ -n_{35z} & 0 \end{bmatrix}$$

$$\begin{bmatrix} a_z - r_{42z} & -a_y + r_{42y} \\ 0 & a_x - r_{42x} \\ -a_x + r_{42x} & 0 \\ 0 & 0 \\ 1 & 0 \\ 0 & 1 \end{bmatrix} \begin{Bmatrix} \dot{d}_{35} \\ \dot{\theta}_{25} \\ \dot{\theta}_{35} \\ \omega_{42x} \\ \omega_{42y} \\ \omega_{42z} \end{Bmatrix} = \begin{Bmatrix} 0 \\ 0 \\ 0 \\ 0 \\ 0 \\ 0 \end{Bmatrix}$$

$$\Rightarrow [A_1] \{\dot{\theta}_a\} + [A_2] \{\Omega\} = 0$$

$$\Rightarrow \{\Omega\} = -[A_2]^{-1} [A_1] \{\dot{\theta}_a\}$$

$$\therefore \{\dot{X}\} = [J] \{\dot{\theta}\} = [J_1] \{\dot{\theta}_a\} + [J_2] \{\Omega\}$$

$$= [J_1] \{\dot{\theta}_a\} - [J_2] [A_2]^{-1} [A_1] \{\dot{\theta}_a\}$$

The elements of $\hat{n}_{ij} = \{n_{ijx} \ n_{ijy} \ n_{ijz}\}^T$ should always satisfy the equation $n_{ijx}^2 + n_{ijy}^2 + n_{ijz}^2 = 1$. For this to be satisfied, the elements are considered as below:

$$\hat{n}_{ij} = \begin{Bmatrix} n_{ijx} \\ n_{ijy} \\ n_{ijz} \end{Bmatrix} = \begin{Bmatrix} \sin(\beta_{ij}) \cos(\phi_{ij}) \\ \sin(\beta_{ij}) \sin(\phi_{ij}) \\ \cos(\beta_{ij}) \end{Bmatrix}$$

For the chosen end-effector location $\vec{a} = \{3 \ 4 \ 5\}^T$, the matrices $[J_1]$, $[J_2]$, $[A_1]$ and $[A_2]$ would finally be

$$[J_1] = \begin{bmatrix} -(4 - r_{13y}) \cos(\beta_{13}) + (5 - r_{13z}) \sin(\phi_{13}) \sin(\beta_{13}) & 0 \\ (3 - r_{13x}) \cos(\beta_{13}) - (5 - r_{13z}) \sin(\beta_{13}) \cos(\phi_{13}) & 0 \\ -(3 - r_{13x}) \sin(\phi_{13}) \sin(\beta_{13}) + (4 - r_{13y}) \sin(\beta_{13}) \cos(\phi_{13}) & 0 \\ \sin(\beta_{13}) \cos(\phi_{13}) & 0 \\ \sin(\phi_{13}) \sin(\beta_{13}) & 0 \\ \cos(\beta_{13}) & 0 \end{bmatrix}$$

$$[J_2] = \begin{bmatrix} \sin(\beta_{35}) \cos(\phi_{35}) & 0 \\ \sin(\phi_{35}) \sin(\beta_{35}) & 0 \\ \cos(\beta_{35}) & 0 \\ 0 & 0 \\ 0 & 0 \\ 0 & 0 \end{bmatrix}$$

$$\begin{bmatrix} -(4 - r_{35y}) \cos(\beta_{35}) + (5 - r_{35z}) \sin(\phi_{35}) \sin(\beta_{35}) \\ (3 - r_{35x}) \cos(\beta_{35}) - (5 - r_{35z}) \sin(\beta_{35}) \cos(\phi_{35}) \\ -(3 - r_{35x}) \sin(\phi_{35}) \sin(\beta_{35}) + (4 - r_{35y}) \sin(\beta_{35}) \cos(\phi_{35}) \\ \sin(\beta_{35}) \cos(\phi_{35}) \\ \sin(\phi_{35}) \sin(\beta_{35}) \\ \cos(\beta_{35}) \end{bmatrix}$$

$$\begin{bmatrix} 0 & 0 & 0 \\ 0 & 0 & 0 \\ 0 & 0 & 0 \\ 0 & 0 & 0 \\ 0 & 0 & 0 \\ 0 & 0 & 0 \end{bmatrix}$$

$$[A_1] = \begin{bmatrix} (4 - r_{13y}) \cos(\beta_{13}) - (5 - r_{13z}) \sin(\phi_{13}) \sin(\beta_{13}) \\ -(3 - r_{13x}) \cos(\beta_{13}) + (5 - r_{13z}) \sin(\beta_{13}) \cos(\phi_{13}) \\ (3 - r_{13x}) \sin(\phi_{13}) \sin(\beta_{13}) - (4 - r_{13y}) \sin(\beta_{13}) \cos(\phi_{13}) \\ -\sin(\beta_{13}) \cos(\phi_{13}) \\ -\sin(\phi_{13}) \sin(\beta_{13}) \\ -\cos(\beta_{13}) \\ -(4 - r_{14y}) \cos(\beta_{14}) + (5 - r_{14z}) \sin(\phi_{14}) \sin(\beta_{14}) \\ (3 - r_{14x}) \cos(\beta_{14}) - (5 - r_{14z}) \sin(\beta_{14}) \cos(\phi_{14}) \\ -(3 - r_{14x}) \sin(\phi_{14}) \sin(\beta_{14}) + (4 - r_{14y}) \sin(\beta_{14}) \cos(\phi_{14}) \\ \sin(\beta_{14}) \cos(\phi_{14}) \\ \sin(\phi_{14}) \sin(\beta_{14}) \\ \cos(\beta_{14}) \end{bmatrix}$$

$$[A_2] = \begin{bmatrix} -\sin(\beta_{35}) \cos(\phi_{35}) \\ -\sin(\phi_{35}) \sin(\beta_{35}) \\ -\cos(\beta_{35}) \\ 0 \\ 0 \\ 0 \end{bmatrix}$$

$$\begin{bmatrix} -(4 - r_{25y}) \cos(\beta_{25}) + (5 - r_{25z}) \sin(\phi_{25}) \sin(\beta_{25}) \\ (3 - r_{25x}) \cos(\beta_{25}) - (5 - r_{25z}) \sin(\beta_{25}) \cos(\phi_{25}) \\ -(3 - r_{25x}) \sin(\phi_{25}) \sin(\beta_{25}) + (4 - r_{25y}) \sin(\beta_{25}) \cos(\phi_{25}) \\ \sin(\beta_{25}) \cos(\phi_{25}) \\ \sin(\phi_{25}) \sin(\beta_{25}) \\ \cos(\beta_{25}) \\ (4 - r_{35y}) \cos(\beta_{35}) - (5 - r_{35z}) \sin(\phi_{35}) \sin(\beta_{35}) \\ -(3 - r_{35x}) \cos(\beta_{35}) + (5 - r_{35z}) \sin(\beta_{35}) \cos(\phi_{35}) \\ (3 - r_{35x}) \sin(\phi_{35}) \sin(\beta_{35}) - (4 - r_{35y}) \sin(\beta_{35}) \cos(\phi_{35}) \\ -\sin(\beta_{35}) \cos(\phi_{35}) \\ -\sin(\phi_{35}) \sin(\beta_{35}) \\ -\cos(\beta_{35}) \end{bmatrix}$$

$$\begin{bmatrix} 0 & 5 - r_{42z} & r_{42y} - 4 \\ r_{42z} - 5 & 0 & 3 - r_{42x} \\ 4 - r_{42y} & r_{42x} - 3 & 0 \\ 1 & 0 & 0 \\ 0 & 1 & 0 \\ 0 & 0 & 1 \end{bmatrix}$$

By using the matrices $[J_1]$, $[J_2]$, $[A_1]$ and $[A_2]$, the relation between the active joint velocities and the end-effector velocities can be written as

$$\{\dot{X}\} = \left([J_1] - [J_2] [A_2]^{-1} [A_1] \right) \{\dot{\theta}_a\} = [\tilde{J}] \{\dot{\theta}_a\}$$

where $[\tilde{J}] = [J_1] - [J_2] [A_2]^{-1} [A_1]$ is the Jacobian matrix of the manipulator for the considered actuating joints.

Therefore, the formulation of the optimisation problem would then be

Maximise

$$f_1 = \sqrt{\det \left(\begin{bmatrix} \tilde{J}^T & \tilde{J} \end{bmatrix} \right)}$$

subject to the bounds

$$\begin{aligned} 0 &\leq r_{ijk} \leq 10, \\ 0 &\leq \beta_{ij} \leq \pi, \\ 0 &\leq \phi_{ij} \leq 2\pi. \end{aligned}$$

Based on the strategy mentioned in section 3.4, the above optimisation problem is attempted for solution, but it did not pass the criterion mentioned in Step 1. Hence, the modified objective function is taken for optimisation in order to avoid type-2 singularity. The modified optimisation problem would then become

Maximise

$$f_2 = \sqrt{\det \left(\begin{bmatrix} \tilde{A}^T & \tilde{A} \end{bmatrix} \right) \times \det \left(\begin{bmatrix} \tilde{B}^T & \tilde{B} \end{bmatrix} \right)}$$

subject to the bounds

$$\begin{aligned} 0 &\leq r_{ijk} \leq 10, \\ 0 &\leq \beta_{ij} \leq \pi, \\ 0 &\leq \phi_{ij} \leq 2\pi, \end{aligned}$$

Condition number formulation:

Scaled Jacobian matrix is formulated based on the methodology explained in section 3.2, as shown below.

The effective distances are formulated as follows.

$$\begin{aligned} \bar{d}_1 &= |(\vec{r}_{13} - \vec{a}) \times \hat{n}_{13}| \\ \bar{d}_2 &= |(\vec{r}_{14} - \vec{a}) \times \hat{n}_{14}| \\ \bar{d}_3 &= |(\vec{r}_{25} - \vec{a}) \times \hat{n}_{25}| \\ \bar{d}_4 &= |(\vec{r}_{35} - \vec{a}) \times \hat{n}_{35}| \\ \bar{d}_5 &= |\vec{r}_{42} - \vec{a}| \end{aligned}$$

The characteristic length is formulated as follows.

$$L = \frac{\bar{d}_1 + \bar{d}_2 + \bar{d}_3 + \bar{d}_4 + \bar{d}_5}{5}$$

By using the above characteristic length, the scaling matrix [S] can be calculated as follows.

$$[S] = \begin{bmatrix} \frac{1}{L} & 0 & 0 & 0 & 0 & 0 \\ 0 & \frac{1}{L} & 0 & 0 & 0 & 0 \\ 0 & 0 & \frac{1}{L} & 0 & 0 & 0 \\ 0 & 0 & 0 & 1 & 0 & 0 \\ 0 & 0 & 0 & 0 & 1 & 0 \\ 0 & 0 & 0 & 0 & 0 & 1 \end{bmatrix}$$

The scaled Jacobian matrix can then be calculated as

$$[\tilde{J}_s] = [S] [\tilde{J}]$$

The condition number of $[\tilde{J}_s]$ is used for comparison.

Variable	Value
ϕ_{13}	360.0°
ϕ_{14}	104.74°
ϕ_{25}	347.83°
ϕ_{35}	32.44°
r_{13x}	10.0
r_{13y}	10.0
r_{13z}	10.0
r_{14x}	10.0
r_{14y}	10.0
r_{14z}	0.0
r_{42x}	10.0
r_{42y}	0.0
r_{42z}	10.0
r_{25x}	0.0
r_{25y}	0.0
r_{25z}	0.0
r_{35x}	0.0
r_{35y}	10.0
r_{35z}	0.0
β_{13}	137.39°
β_{14}	45.96°
β_{25}	134.35°
β_{35}	68.46°

Table 3. Result of the optimisation problem corresponding to 2D-M71 manipulator.

Result of the optimisation problem:

Solution to the optimisation problem is shown in Table 3 (with the values rounded up to two decimal places).

Therefore, the locations and orientations of the joints are shown below.

$$\begin{aligned} \hat{n}_{13} &= -0.0\hat{i} + 0.68\hat{j} - 0.74\hat{k} \\ \hat{n}_{14} &= 0.7\hat{i} - 0.18\hat{j} + 0.7\hat{k} \\ \hat{n}_{25} &= -0.15\hat{i} + 0.7\hat{j} - 0.7\hat{k} \\ \hat{n}_{35} &= 0.5\hat{i} + 0.78\hat{j} + 0.37\hat{k} \\ \vec{r}_{13} &= 10.0\hat{i} + 10.0\hat{j} + 10.0\hat{k} \\ \vec{r}_{14} &= 10.0\hat{i} + 10.0\hat{j} + 0.0\hat{k} \\ \vec{r}_{42} &= 10.0\hat{i} + 0.0\hat{j} + 10.0\hat{k} \\ \vec{r}_{25} &= 0.0\hat{i} + 0.0\hat{j} + 0.0\hat{k} \\ \vec{r}_{35} &= 0.0\hat{i} + 10.0\hat{j} + 0.0\hat{k} \end{aligned}$$

The corresponding optimum manipulability is given by

$$\mu = 173.16$$

And the corresponding condition number is

$$\kappa = 1.98$$

And the corresponding scaled manipulability index, which is the product of singular values of the scaled Jacobian $[\tilde{J}_s]$, is

$$\bar{\mu} = 0.2305$$

Similarly, manipulability indices and condition numbers (wherever applicable) for all the other manipulators are computed, and finally the prescriptions for 1-DOF, 2-DOF, 3-DOF and 4-DOF manipulators for optimal performance around the task point $\vec{a} = \{1, 2, 3\}^T$ are presented below.

4.2 Prescriptions

A list of manipulators with their manipulability indices (μ) and the corresponding scaled manipulability indices ($\bar{\mu}$), is presented for each of 1-DOF, 2-DOF, 3-DOF and 4-DOF manipulators, in which the manipulators are sorted by scaled manipulability index in the descending order. For manipulators with more than 1-DOF, the corresponding condition numbers (κ) and the corresponding indices i_κ are also shown. The corresponding objective function used in optimisation is also shown with the name f . The designation $f = f_1$ implies

that the objective function used is $f_1 = \sqrt{\det \left(\begin{bmatrix} \tilde{J} \\ \tilde{J} \end{bmatrix}^T \begin{bmatrix} \tilde{J} \\ \tilde{J} \end{bmatrix} \right)}$ and

the designation $f = f_2$ implies that the objective function used is $f_2 = \sqrt{\det \left(\begin{bmatrix} \tilde{A} \\ \tilde{A} \end{bmatrix}^T \begin{bmatrix} \tilde{A} \\ \tilde{A} \end{bmatrix} \right) \times \det \left(\begin{bmatrix} \tilde{B} \\ \tilde{B} \end{bmatrix}^T \begin{bmatrix} \tilde{B} \\ \tilde{B} \end{bmatrix} \right)}$.

4.2.1 Prescription for 1-DOF manipulators

The prescription containing 96 1-DOF manipulators is shown in table 2. The last column, namely AJV (Active Joint Velocities), shows the joints that are considered to be actuating joints for the closed-loop manipulators. Since all the manipulators considered in this section are single-degree-of-freedom manipulators, the condition number of every manipulator would be 1 and hence the condition numbers are not shown in this prescription.

S.No.	Name	$\bar{\mu}$	μ	f	AJV
1	1D-M10	0.1523	8.1	f_1	θ_{14}
2	1D-M65	0.1376	10.5	f_2	θ_{14}
3	1D-M8	0.1152	7.1	f_1	θ_{14}
4	1D-M94	0.1106	1.0	f_2	d_{24}
5	1D-M28	0.1088	8.1	f_1	θ_{14}
6	1D-M20	0.0824	10.5	f_1	θ_{14}
7	1D-M34	0.0798	7.1	f_1	θ_{14}
8	1D-M95	0.0776	1.0	f_2	d_{12}
9	1D-M7	0.0774	8.4	f_1	θ_{14}
10	1D-M29	0.0732	10.5	f_1	θ_{14}
11	1D-M41	0.0722	9.5	f_1	θ_{14}
12	1D-M40	0.071	7.1	f_1	θ_{14}
13	1D-M35	0.0706	10.5	f_1	θ_{14}
14	1D-M11	0.062	10.5	f_1	θ_{14}
15	1D-M64	0.0563	20.3	f_2	θ_{13}
16	1D-M66	0.0487	19.8	f_2	θ_{23}
17	1D-M60	0.0475	8.4	f_1	θ_{14}
18	1D-M93	0.0467	1.0	f_2	d_{23}
19	1D-M59	0.0462	9.5	f_1	θ_{14}
20	1D-M91	0.0438	1.0	f_2	d_{13}
21	1D-M79	0.0335	1	f_1	d_{14}
22	1D-M25	0.0313	17.3	f_2	θ_{13}

...continued

continuing...

S.No.	Name	$\bar{\mu}$	μ	f	AJV
23	1D-M44	0.0313	17.3	f_2	θ_{23}
24	1D-M67	0.0306	18.3	f_2	θ_{24}
25	1D-M15	0.0305	21.2	f_2	θ_{12}
26	1D-M22	0.0246	17.3	f_2	θ_{13}
27	1D-M13	0.024	15.3	f_2	θ_{12}
28	1D-M46	0.0237	15.3	f_2	θ_{12}
29	1D-M45	0.0229	17.3	f_2	θ_{24}
30	1D-M3	0.0222	15.4	f_2	θ_{13}
31	1D-M49	0.0219	14.1	f_2	θ_{12}
32	1D-M68	0.0214	19.6	f_2	θ_{12}
33	1D-M5	0.0212	14.7	f_2	θ_{13}
34	1D-M47	0.0212	17.3	f_2	θ_{12}
35	1D-M24	0.0212	17.3	f_2	θ_{13}
36	1D-M51	0.0203	14.9	f_2	θ_{12}
37	1D-M18	0.0194	14.6	f_2	θ_{24}
38	1D-M69	0.019	19.0	f_2	θ_{24}
39	1D-M48	0.0189	14.0	f_2	θ_{12}
40	1D-M12	0.0188	12.8	f_2	θ_{23}
41	1D-M9	0.0185	12.8	f_2	θ_{23}
42	1D-M23	0.0177	13.0	f_2	θ_{13}
43	1D-M62	0.0167	9.6	f_2	θ_{12}
44	1D-M26	0.0167	9.6	f_2	θ_{13}
45	1D-M14	0.0163	10.1	f_2	θ_{12}
46	1D-M96	0.016	1.0	f_2	d_{24}
47	1D-M6	0.0159	12.0	f_2	θ_{13}
48	1D-M4	0.0158	13.4	f_2	θ_{13}
49	1D-M89	0.0155	1	f_1	d_{14}
50	1D-M38	0.0153	12.9	f_2	θ_{23}
51	1D-M58	0.0148	8.2	f_2	θ_{13}
52	1D-M57	0.0143	11.7	f_2	θ_{34}
53	1D-M76	0.0138	1	f_1	d_{14}
54	1D-M17	0.0136	8.6	f_2	θ_{12}
55	1D-M50	0.0135	11.1	f_2	θ_{12}
56	1D-M19	0.0134	10.3	f_2	θ_{13}
57	1D-M56	0.0129	10.5	f_2	θ_{24}
58	1D-M21	0.0128	10.5	f_2	θ_{12}
59	1D-M27	0.0127	9.3	f_2	θ_{13}
60	1D-M77	0.0126	1	f_1	d_{14}
61	1D-M16	0.0125	9.3	f_2	θ_{12}
62	1D-M2	0.0116	6.7	f_2	θ_{13}
63	1D-M1	0.0113	8.4	f_2	θ_{13}
64	1D-M43	0.0108	1	f_1	d_{14}
65	1D-M39	0.01	8.5	f_2	θ_{24}
66	1D-M80	0.0082	1	f_1	d_{14}
67	1D-M36	0.0081	1	f_1	d_{14}
68	1D-M92	0.0071	1	f_1	d_{14}
69	1D-M61	0.0051	1	f_1	d_{14}
70	1D-M42	0.0034	1	f_1	d_{14}
71	1D-M31	0.0031	1.7	f_2	d_{13}
72	1D-M37	0.0025	1	f_1	d_{14}
73	1D-M86	0.0021	1.0	f_2	d_{12}
74	1D-M30	0.002	1.1	f_2	d_{13}
75	1D-M53	0.0017	1.1	f_2	d_{12}
76	1D-M83	0.0016	1.0	f_2	d_{12}
77	1D-M84	0.0015	1.0	f_2	d_{12}
78	1D-M87	0.0015	1.0	f_2	d_{24}
79	1D-M55	0.0015	1.3	f_2	d_{12}

...continued

continuing...					
S.No.	Name	$\bar{\mu}$	μ	f	AJV
80	1D-M71	0.0015	1.0	f_2	d_{13}
81	1D-M73	0.0015	1.0	f_2	d_{13}
82	1D-M90	0.0015	1.0	f_2	d_{12}
83	1D-M52	0.0015	1.1	f_2	d_{12}
84	1D-M82	0.0014	1.0	f_2	d_{12}
85	1D-M72	0.0014	1	f_2	d_{13}
86	1D-M70	0.0014	1.0	f_2	d_{13}
87	1D-M81	0.0014	1	f_2	d_{23}
88	1D-M85	0.0014	1.0	f_2	d_{12}
89	1D-M88	0.0014	1.0	f_2	d_{13}
90	1D-M63	0.0013	1.1	f_2	d_{12}
91	1D-M32	0.0013	0.7	f_2	d_{13}
92	1D-M54	0.0013	1.1	f_2	d_{12}
93	1D-M33	0.0012	0.8	f_2	d_{13}
94	1D-M78	0.0009	0.6	f_2	d_{23}
95	1D-M74	0.0008	0.6	f_2	d_{13}
96	1D-M75	0.0006	0.4	f_2	d_{13}

Table 4. Prescription of 1-DOF Manipulators.

This prescription gives the designer the set of 1-DOF manipulators arranged in descending order of performance of manipulators to operate around the end-effector point $\vec{a} = \{3, 4, 5\}^T$.

4.2.2 Prescription for 2-DOF manipulators

A contracted version of the prescription containing 645 1-DOF manipulators is shown in table 3. Full table is shown in appendix A, in which the actuating joint velocities (AJV) considered for this study are shown. In the table, κ refers to the condition number of the Jacobian at the optimum point and i_κ refers to the ranked position of the manipulator based on its condition number.

S.No.	Name	$\bar{\mu}$	κ	i_κ	μ	f
1	2D-M645	1.0	1.0	6	1.0	f_1
2	2D-M315	0.7544	1.2	155	87.4	f_1
3	2D-M301	0.7058	1.2	158	88.8	f_2
4	2D-M224	0.6366	1.1	127	60.2	f_1
5	2D-M308	0.6034	1.1	118	340.6	f_2
6	2D-M126	0.5855	1.3	207	88.8	f_1
7	2D-M309	0.5624	1.2	135	351.6	f_2
8	2D-M319	0.5621	1.4	230	283.4	f_2
9	2D-M208	0.5495	1.2	172	68.1	f_1
10	2D-M134	0.541	1.1	107	100.5	f_1
11	2D-M248	0.5381	1.4	224	75.2	f_1
12	2D-M203	0.5289	1.3	198	68.1	f_1
13	2D-M634	0.5142	1.0	7	1	f_1
14	2D-M458	0.5116	1.0	32	1.0	f_1
15	2D-M74	0.5114	1.1	115	77.5	f_1
\vdots	\vdots	\vdots	\vdots	\vdots	\vdots	\vdots
641	2D-M579	0.0007	1.4	243	0.5	f_2
642	2D-M591	0.0007	1.4	256	0.5	f_2

...continued

continuing...						
S.No.	Name	$\bar{\mu}$	κ	i_κ	μ	f
643	2D-M572	0.0007	1.4	239	0.5	f_2
644	2D-M491	0.0007	1.3	203	0.5	f_2
645	2D-M607	0.0006	1.6	282	0.4	f_2

Table 5. Prescription of 2-DOF Manipulators.

This prescription gives the designer the set of 2-DOF manipulators arranged in descending order of performance of manipulators to operate around the end-effector point $\vec{a} = \{3, 4, 5\}^T$.

4.2.3 Prescription for 3-DOF manipulators

The prescription containing 8 3-DOF manipulators is shown in table 6. All the eight manipulators happened to be serial manipulators and hence the objective function f is f_1 for all the 8 manipulators. Since all the 3-DOF manipulators here are serial manipulators, all the joints would be actuating joints, and hence the AJV column is not shown in the table.

S.No.	Name	$\bar{\mu}$	κ	i_κ	μ	f
1	3D-M1	1.0113	1.5	2	1058.9	f_1
2	3D-M8	1.0	1.0	1	1.0	f_1
3	3D-M2	0.0962	14.8	4	111.0	f_1
4	3D-M3	0.0962	15.5	8	111.0	f_1
5	3D-M4	0.0962	14.8	7	111.0	f_1
6	3D-M7	0.0091	14.8	5	10.5	f_1
7	3D-M5	0.0091	14.8	6	10.5	f_1
8	3D-M6	0.0091	14.8	3	10.5	f_1

Table 6. Prescription of 3-DOF Manipulators.

This prescription gives the designer the set of 3-DOF manipulators arranged in descending order of performance of manipulators to operate around the end-effector point $\vec{a} = \{3, 4, 5\}^T$.

4.2.4 Prescription for 4-DOF manipulators

The prescription containing 15 4-DOF manipulators is shown in table 6. All the 15 manipulators also happened to be serial manipulators and hence the objective function f is f_1 for all the manipulators. Since all these manipulators are serial manipulators, all the joints would be actuating joints, and hence the AJV column is not shown in the table.

This prescription gives the designer the set of 4-DOF manipulators arranged in descending order of performance of manipulators to operate around the end-effector point $\vec{a} = \{3, 4, 5\}^T$.

5 Discussions

5.1 On the prescription for manipulators of DOF 1

The manipulator with the highest scaled manipulability is 1D-M10 with $\bar{\mu} = 0.1523$ and the corresponding dimensional parameters from the corresponding optimisation result are

S.No.	Name	$\bar{\mu}$	κ	i_κ	μ	f
1	4D-M1	2.5607	1.5	1	2074.5	f_1
2	4D-M13	0.4866	3.0	2	1.0	f_1
3	4D-M12	0.4048	3.1	3	1	f_1
4	4D-M4	0.2619	15.3	14	211.0	f_1
5	4D-M5	0.2619	15.3	13	211.0	f_1
6	4D-M2	0.2619	15.3	12	211.0	f_1
7	4D-M3	0.2619	15.3	15	211.0	f_1
8	4D-M15	0.077	4.9	4	1.0	f_1
9	4D-M14	0.0538	5.5	5	1.0	f_1
10	4D-M9	0.0253	12.9	7	17.6	f_1
11	4D-M11	0.0253	12.9	10	17.6	f_1
12	4D-M10	0.0253	12.9	6	17.6	f_1
13	4D-M7	0.0253	12.9	8	17.6	f_1
14	4D-M8	0.0253	12.9	9	17.6	f_1
15	4D-M6	0.0253	12.9	11	17.6	f_1

Table 7. Prescription of 4-DOF Manipulators.

$$\begin{aligned}
\hat{n}_{14} &= -\hat{k} \\
\hat{n}_{23} &= 0.04\hat{i} - 0.71\hat{j} + 0.7\hat{k} \\
\hat{n}_{24} &= -0.84\hat{i} - 0.49\hat{j} - 0.25\hat{k} \\
\vec{r}_{13} &= 3.76\hat{i} + 5.51\hat{j} + 5.34\hat{k} \\
\vec{r}_{14} &= 10\hat{i} + 1.6\hat{k} \\
\vec{r}_{23} &= 4.11\hat{i} + 6.4\hat{j} + 4.81\hat{k} \\
\vec{r}_{24} &= 4.67\hat{i} + 3.62\hat{j} + 5.9\hat{k}
\end{aligned}$$

From the above data, the link lengths can be derived as follows.

$$\begin{aligned}
l_1 &= |\vec{r}_{13} - \vec{r}_{14}| = 9.13 \\
l_2 &= |\vec{r}_{23} - \vec{r}_{24}| = 3.04 \\
l_3 &= |\vec{r}_{13} - \vec{r}_{23}| = 1.09 \\
l_{4a} &= |\vec{r}_{14} - \vec{r}_{24}| = 7.75 \\
l_{4b} &= |\vec{r}_{14} - \vec{a}| = 8.75 \\
l_{4c} &= |\vec{r}_{24} - \vec{a}| = 1.94
\end{aligned}$$

Hence, the first link should have a length of 9.13m, the second link should have a length of 3.04m, the third link should have a length of 1.09m, and the fourth link, if assumed to be of triangular shape, should have its sides 7.75m, 8.75m and 1.94m, wherein the sides of lengths 8.75m and 1.94m meet at the end-effector point, and the side of length 7.75m connects the end-effector and the revolute joint.

The revolute joint connecting the links 2 and 3 is to be located at (4.11, 6.4, 4.81) with its axis oriented along the unit vector $0.04\hat{i} - 0.71\hat{j} + 0.7\hat{k}$. The other revolute joint is to be located at (10, 0, 1.6) with its axis oriented along the unit vector $-\hat{k}$. The cylindrical joint is to be located at (4.67, 3.62, 5.9) with its axis oriented along the unit vector $-0.84\hat{i} - 0.49\hat{j} - 0.25\hat{k}$. Finally, the spherical joint is to be located at (3.76, 5.51, 5.34).

If the designer, for some other constraints, is not interested in this particular type of manipulator, i.e., 1D-M10, the prescription provides the next best manipulator, i.e., 1D-M65,

for which the corresponding dimensional parameters are available. This gives the designer the set of 1-DOF manipulators to choose the manipulator from, with the appropriate dimensions that are necessary to build the manipulator.

5.2 On the prescription for manipulators of DOF 2

The manipulator with the highest scaled manipulability is 2D-M645 with $\bar{\mu} = 1.0$ and the corresponding dimensional parameters are

$$\begin{aligned}
\hat{n}_{12} &= 0.97\hat{i} + 0.03\hat{j} + 0.24\hat{k} \\
\hat{n}_{23} &= 0.03\hat{i} - 1.0\hat{j} - 0.01\hat{k}
\end{aligned}$$

This shows that the axis of the prismatic joint connecting the links 1 and 2 is to be along the unit vector $0.97\hat{i} + 0.03\hat{j} + 0.24\hat{k}$ and the axis of the prismatic joint connecting the links 2 and 3 is to be along the unit vector $0.03\hat{i} - 1.0\hat{j} - 0.01\hat{k}$.

In the optimised result, there are no specified locations for the prismatic joints. This is because the Jacobian is not dependent on the locations of prismatic joints, as a prismatic joint can give the same velocity regardless of the location of its joint, as long as its axis is unchanged. Hence, the parameters corresponding to locations of the prismatic joints, i.e., the components of the position vectors \vec{r}_{12} and \vec{r}_{23} , are free parameters that can be chosen by the designer within the specified bounds.

For any reason if the designer does not opt for this particular type of manipulator, i.e., 2D-M645, the next best manipulator is provided in the prescription, which is 2D-M315, along with the corresponding dimensional parameters from the optimisation results. This gives the designer the list of 2-DOF manipulators to choose the manipulator from, with the appropriate dimensional parameters that are essential to build the manipulator.

5.3 On the prescription for manipulators of DOF 3

The manipulator with the highest scaled manipulability is 3D-M1 with $\bar{\mu} = 1.0113$ and the corresponding dimensional parameters are

$$\begin{aligned}
\hat{n}_{13} &= -0.71\hat{i} + 0.11\hat{j} - 0.7\hat{k} \\
\hat{n}_{23} &= -0.0\hat{i} + 0.58\hat{j} - 0.81\hat{k} \\
\hat{n}_{24} &= 0.82\hat{i} - 0.46\hat{j} - 0.34\hat{k} \\
\vec{r}_{13} &= 10.0\hat{i} + 10.0\hat{j} + 0.0\hat{k} \\
\vec{r}_{23} &= 10.0\hat{i} + 0.0\hat{j} + 10.0\hat{k} \\
\vec{r}_{24} &= 10.0\hat{i} + 10.0\hat{j} + 10.0\hat{k}
\end{aligned}$$

From the above data, the link lengths can be derived as follows.

$$\begin{aligned}
l_2 &= |\vec{r}_{23} - \vec{r}_{24}| = 14.14 \\
l_3 &= |\vec{r}_{13} - \vec{r}_{23}| = 10.0 \\
l_4 &= |\vec{a} - \vec{r}_{24}| = 10.49
\end{aligned}$$

Hence, the second link should have a length of 14.14m, the third link should have a length of 10.0m, and the fourth link should have a length of 10.49m.

The revolute joint connecting the links 1 and 3 is to be located at (10.0, 10.0, 0.0) with its axis oriented along the unit vector $-0.71\hat{i} + 0.11\hat{j} - 0.7\hat{k}$. The revolute joint connecting the links 2 and 3 is to be located at (10.0, 0.0, 10.0) with its axis oriented along the unit vector $0.0\hat{i} + 0.58\hat{j} - 0.81\hat{k}$. And the revolute joint connecting the links 2 and 4 is to be located at (10.0, 10.0, 10.0) with its axis oriented along the unit vector $0.82\hat{i} - 0.46\hat{j} - 0.34\hat{k}$.

If the designer due to some other restrictions does not find the manipulator 3D-M1 viable, the next best manipulator, i.e., 3D-M8, is available in the prescription, with its corresponding dimensional parameters. This gives the designer an atlas of 3-DOF manipulators to choose the manipulator from, with the appropriate dimensional parameters that are necessary to build the manipulator.

5.4 On the prescription for manipulators of DOF 4

The manipulator with the highest scaled manipulability is 4D-M1 with $\bar{\mu} = 2.5607$ and the corresponding dimensional parameters are

$$\begin{aligned}\hat{n}_{14} &= -0.29\hat{i} + 0.57\hat{j} - 0.77\hat{k} \\ \hat{n}_{23} &= 0.75\hat{i} - 0.53\hat{j} + 0.4\hat{k} \\ \hat{n}_{25} &= -0.34\hat{i} + 0.83\hat{j} - 0.45\hat{k} \\ \hat{n}_{34} &= -0.72\hat{i} + 0.12\hat{j} + 0.69\hat{k} \\ \vec{r}_{14} &= 10.0\hat{i} + 0.0\hat{j} + 10.0\hat{k} \\ \vec{r}_{23} &= 10.0\hat{i} + 10.0\hat{j} + 0.0\hat{k} \\ \vec{r}_{25} &= 0.0\hat{i} + 0.0\hat{j} + 0.0\hat{k} \\ \vec{r}_{34} &= 10.0\hat{i} + 10.0\hat{j} + 10.0\hat{k}\end{aligned}$$

From the above data, the link lengths can be derived as follows.

$$\begin{aligned}l_4 &= |\vec{r}_{14} - \vec{r}_{34}| = 10.0 \\ l_3 &= |\vec{r}_{34} - \vec{r}_{23}| = 10.0 \\ l_2 &= |\vec{r}_{23} - \vec{r}_{25}| = 14.14 \\ l_5 &= |\vec{r}_{25} - \vec{a}| = 7.07\end{aligned}$$

Hence, the second link should have a length of 14.14m, the third link should have a length of 10.0m, the fourth link should have a length of 10.0m, and the fifth link should have a length of 7.07m.

The revolute joint connecting the links 1 and 4 is to be located at (10.0, 0.0, 10.0) with its axis oriented along the unit vector $-0.29\hat{i} + 0.57\hat{j} - 0.77\hat{k}$. The revolute joint connecting the links 3 and 4 is to be located at (10.0, 10.0, 10.0) with its axis oriented along the unit vector $-0.72\hat{i} + 0.12\hat{j} + 0.69\hat{k}$. The revolute joint connecting the links 2 and 3 is to be located at (10.0, 10.0, 0.0) with its axis oriented along the unit vector $0.75\hat{i} - 0.53\hat{j} + 0.4\hat{k}$. And the revolute joint connecting the links 2 and 5 is to be located at (0.0, 0.0, 0.0) with its axis oriented along the unit vector $-0.34\hat{i} + 0.83\hat{j} - 0.45\hat{k}$.

In case the designer could not use 4D-M1 for any other constraint, the prescription provides the next best manipulator, i.e., 4D-M13, with the corresponding dimensional parameters that are available from the optimisation results. This gives the designer the set of 4-DOF manipulators to choose the

manipulator from, with the appropriate dimensions that are required to build the manipulator.

6 Conclusion

Dimensional synthesis is done for 1-DOF, 2-DOF, 3-DOF and 4-DOF manipulators, by optimising the manipulability index around the chosen end-effector point for this study. Condition numbers for 2-DOF, 3-DOF and 4-DOF manipulators are calculated. The DOF-wise performance of the manipulators is compared by using the scaled manipulability indices ($\bar{\mu}$) of the manipulators, and DOF-wise prescriptions are provided for manipulators. For 1-DOF, 1D-M10 is found to have the maximum scaled manipulability index. Among 2-DOF manipulators, 2D-M645 manipulator is found to have the maximum scaled manipulability index and 78 manipulators are found to be having the lowest condition number (rounded up to one decimal point). Among 3-DOF manipulators, 3D-M1 is found to have the maximum scaled manipulability index and 3D-M8 is found to have the lowest condition number. Among 4-DOF manipulators, 4D-M1 is found to have both the highest scaled manipulability index and the lowest condition number.

The manipulator with the most scaled manipulability reflects the best performance around the required task position, provided the condition number is reasonable. In case the designer, due to some other constraints, is not interested in the manipulator with the highest scaled manipulability, the prescription provides the second best manipulator (and, then others ranked appropriately) with its corresponding condition number, if applicable. This, along with the result of the companion study, gives the designer an atlas of manipulators to choose the manipulator from, with the appropriate dimensions that are necessary to build the manipulator to operate around the specified task point.

References

1. Yoshikawa, T. Manipulability of robotic mechanisms. *The international journal Robotics Res.* **4**, 3–9 (1985).
2. Cleary, K. & Uebel, M. Jacobian formulation for a novel 6-dof parallel manipulator. In *Proceedings of the 1994 IEEE International Conference on Robotics and Automation*, 2377–2382 (IEEE, 1994).
3. Kim, D., Chung, W. & Youm, Y. Analytic jacobian of in-parallel manipulators. In *Proceedings 2000 ICRA. Millennium Conference. IEEE International Conference on Robotics and Automation. Symposia Proceedings (Cat. No.00CH37065)*, vol. 3, 2376–2381 vol.3, DOI: [10.1109/ROBOT.2000.846382](https://doi.org/10.1109/ROBOT.2000.846382) (2000).
4. Kim, S.-G. & Ryu, J. New dimensionally homogeneous jacobian matrix formulation by three end-effector points for optimal design of parallel manipulators. *IEEE Transactions on Robotics Autom.* **19**, 731–736 (2003).

5. Pond, G. & Carretero, J. A. Formulating jacobian matrices for the dexterity analysis of parallel manipulators. *Mech. Mach. Theory* **41**, 1505–1519 (2006).
6. Liu, H., Huang, T. & Chetwynd, D. G. A method to formulate a dimensionally homogeneous jacobian of parallel manipulators. *IEEE Transactions on Robotics* **27**, 150–156 (2010).
7. Hu, B. Formulation of unified jacobian for serial-parallel manipulators. *Robotics Comput. Manuf.* **30**, 460–467 (2014).
8. Doty, K., Melchiorri, C., Schwartz, E. & Bonivento, C. Robot manipulability. *IEEE Transactions on Robotics Autom.* **11**, 462–468, DOI: [10.1109/70.388791](https://doi.org/10.1109/70.388791) (1995).
9. Angeles, J. The design of isotropic manipulator architectures in the presence of redundancies. *Int. J. Rob. Res.* **11**, 196–201, DOI: [10.1177/027836499201100303](https://doi.org/10.1177/027836499201100303) (1992).
10. Stocco, L. J., Salcudean, S. E. & Sassani, F. On the use of scaling matrices for task-specific robot design. *IEEE Transactions on Robotics Autom.* **15**, 958–965, DOI: [10.1109/70.795800](https://doi.org/10.1109/70.795800) (1999).
11. Ma, O. & Angeles, J. Optimum architecture design of platform manipulators. In *Fifth International Conference on Advanced Robotics 'Robots in Unstructured Environments*, 1130–1135 vol.2, DOI: [10.1109/ICAR.1991.240404](https://doi.org/10.1109/ICAR.1991.240404) (1991).
12. Lee, J. A study on the manipulability measures for robot manipulators. In *Proceedings of the 1997 IEEE/RSJ International Conference on Intelligent Robot and Systems. Innovative Robotics for Real-World Applications. IROS '97*, vol. 3, 1458–1465 vol.3, DOI: [10.1109/IROS.1997.656551](https://doi.org/10.1109/IROS.1997.656551) (1997).
13. Khezrian, R., Abedloo, E., Farhadmanesh, M. & Moosavian, S. Multi criteria design of a spherical 3-dof parallel manipulator for optimal dynamic performance. In *Robotics and Mechatronics (ICRoM), 2014 Second RSI/ISM International Conference on*, 546–551 (IEEE, 2014).
14. PAPPURI, H. *Enumeration and Dimensional Synthesis of Planar Manipulating Structures for Velocity and Force Transformations*. Master's thesis (2016).
15. Gosselin, C. & Angeles, J. Singularity analysis of closed-loop kinematic chains. *IEEE Transactions on Robotics Autom.* **6**, 281–290, DOI: [10.1109/70.56660](https://doi.org/10.1109/70.56660) (1990).
16. Briot, S. & Arakelian, V. On the Dynamic Properties of Rigid-Link Flexible-Joint Parallel Manipulators in the Presence of Type 2 Singularities. *J. Mech. Robotics* **2**, DOI: [10.1115/1.4001121](https://doi.org/10.1115/1.4001121) (2010). 021004, https://asmedigitalcollection.asme.org/mechanismsrobotics/article-pdf/2/2/021004/5674937/021004_1.pdf.
17. Pagis, G., Bouton, N., Briot, S. & Martinet, P. Enlarging parallel robot workspace through type-2 singularity crossing. *Control. Eng. Pract.* **39**, 1–11, DOI: <https://doi.org/10.1016/j.conengprac.2015.01.009> (2015).
18. Briot, S. & Bonev, I. A. Accuracy analysis of 3-dof planar parallel robots. *Mech. Mach. Theory* **43**, 445–458, DOI: <https://doi.org/10.1016/j.mechmachtheory.2007.04.002> (2008).
19. Hill, R. B., Six, D., Chriette, A., Briot, S. & Martinet, P. Crossing type 2 singularities of parallel robots without pre-planned trajectory with a virtual-constraint-based controller. In *2017 IEEE International Conference on Robotics and Automation (ICRA)*, 6080–6085, DOI: [10.1109/ICRA.2017.7989721](https://doi.org/10.1109/ICRA.2017.7989721) (2017).
20. Koessler, A., Goldsztejn, A., Briot, S. & Bouton, N. Certified detection of parallel robot assembly mode under type 2 singularity crossing trajectories. In *2017 IEEE International Conference on Robotics and Automation (ICRA)*, 6073–6079, DOI: [10.1109/ICRA.2017.7989720](https://doi.org/10.1109/ICRA.2017.7989720) (2017).
21. Pagis, G., Bouton, N., Briot, S. & Martinet, P. Design of a controller for enlarging parallel robots workspace through type 2 singularity crossing. In *2014 IEEE International Conference on Robotics and Automation (ICRA)*, 4249–4255, DOI: [10.1109/ICRA.2014.6907477](https://doi.org/10.1109/ICRA.2014.6907477) (2014).
22. Gosselin, C., Angeles, J. *et al.* Singularity analysis of closed-loop kinematic chains. *IEEE transactions on robotics automation* **6**, 281–290 (1990).
23. Matlab optimization toolbox (2022). The MathWorks, Natick, MA, USA.
24. Jacob, A. S., Dasgupta, B. & Datta, R. Enumeration of spatial manipulators by using the concept of adjacency matrix, DOI: [10.48550/ARXIV.2210.03327](https://doi.org/10.48550/ARXIV.2210.03327) (2022).

Appendix A

S.No.	Name	$\tilde{\mu}$	κ	i_{κ}	μ	f	AJV
1	2D-M645	1.0	1.0	6	1.0	f_1	d_{12}, d_{23}
2	2D-M315	0.7544	1.2	155	87.4	f_1	θ_{13}, θ_{35}
3	2D-M301	0.7058	1.2	158	88.8	f_2	θ_{14}, θ_{35}
4	2D-M224	0.6366	1.1	127	60.2	f_1	θ_{13}, θ_{35}
5	2D-M308	0.6034	1.1	118	340.6	f_2	θ_{13}, θ_{14}
6	2D-M126	0.5855	1.3	207	88.8	f_1	θ_{14}, θ_{45}
7	2D-M309	0.5624	1.2	135	351.6	f_2	θ_{13}, θ_{24}
8	2D-M319	0.5621	1.4	230	283.4	f_2	θ_{25}, θ_{35}
9	2D-M208	0.5495	1.2	172	68.1	f_1	θ_{13}, θ_{35}
10	2D-M134	0.541	1.1	107	100.5	f_1	θ_{14}, θ_{45}
11	2D-M248	0.5381	1.4	224	75.2	f_1	θ_{13}, θ_{35}
12	2D-M203	0.5289	1.3	198	68.1	f_1	θ_{13}, θ_{35}
13	2D-M634	0.5142	1.0	7	1	f_1	d_{13}, d_{35}
14	2D-M458	0.5116	1.0	32	1.0	f_1	d_{13}, d_{35}
15	2D-M74	0.5114	1.1	115	77.5	f_1	θ_{13}, θ_{35}
16	2D-M318	0.5006	1.1	130	298.9	f_2	θ_{24}, θ_{35}
17	2D-M213	0.4948	1.3	183	60.2	f_1	θ_{13}, θ_{35}
18	2D-M304	0.4879	1.8	307	165.1	f_2	θ_{14}, θ_{24}
19	2D-M311	0.485	1.2	152	88.5	f_1	θ_{13}, θ_{35}
20	2D-M300	0.4831	2.1	316	144.2	f_2	θ_{14}, θ_{34}
21	2D-M314	0.4683	1.2	141	266.1	f_2	θ_{13}, θ_{45}
22	2D-M303	0.4571	1.6	294	181.6	f_2	θ_{14}, θ_{35}
23	2D-M305	0.4477	1.5	266	200.5	f_2	θ_{23}, θ_{35}
24	2D-M98	0.4435	1.3	180	88.8	f_1	θ_{13}, θ_{35}
25	2D-M302	0.4376	1.8	306	164.6	f_2	θ_{14}, θ_{33}

...continued

continuing... Table with columns: S.No., Name, mu, kappa, i_k, mu, f, AVJ. Rows 26-132. Includes values for mu, kappa, i_k, mu, f, and AVJ for various 2D-M models.

continuing... Table with columns: S.No., Name, mu, kappa, i_k, mu, f, AVJ. Rows 133-239. Includes values for mu, kappa, i_k, mu, f, and AVJ for various 2D-M models.

continuing...							
S.No.	Name	μ	κ	i_{κ}	μ	f	AJV
240	2D-M541	0.1172	9.3	345	8.4	f ₁	d ₁₃ , ₀₃₅
241	2D-M249	0.117	1.5	278	95.3	f ₂	θ ₁₃ , ₀₃₅
242	2D-M78	0.1165	1.1	113	68.5	f ₂	θ ₁₃ , ₀₃₅
243	2D-M70	0.1162	1.1	101	57.4	f ₂	θ ₁₃ , ₀₃₄
244	2D-M530	0.1158	17.4	599	17.4	f ₂	d ₁₄ , ₀₁₃
245	2D-M58	0.1149	1.3	214	63.5	f ₂	θ ₁₄ , ₀₃₄
246	2D-M93	0.1146	1.5	273	88.8	f ₂	θ ₁₃ , ₀₃₄
247	2D-M125	0.1145	1.5	260	78.1	f ₂	θ ₁₄ , ₀₃₄
248	2D-M10	0.1143	1.7	302	86.0	f ₂	θ ₁₄ , ₀₃₄
249	2D-M112	0.1143	1.3	194	72.4	f ₂	θ ₁₄ , ₀₂₅
250	2D-M15	0.1138	1.7	303	86.0	f ₂	θ ₁₃ , ₀₁₄
251	2D-M149	0.1138	1.0	74	72.9	f ₂	θ ₁₄ , ₀₂₅
252	2D-M147	0.1138	1.0	73	72.9	f ₂	θ ₁₄ , ₀₂₃
253	2D-M294	0.1137	1.5	258	85.6	f ₂	θ ₂₄ , ₀₄₅
254	2D-M178	0.1129	1.1	96	77.5	f ₂	θ ₂₃ , ₀₃₄
255	2D-M551	0.1124	17.4	598	17.4	f ₂	d ₂₄ , ₀₃₅
256	2D-M123	0.1121	1.2	160	75.2	f ₂	θ ₁₄ , ₀₂₅
257	2D-M2	0.1115	1.2	159	100.4	f ₂	θ ₁₄ , ₀₂₅
258	2D-M119	0.1105	1.3	215	68.1	f ₂	θ ₁₄ , ₀₂₃
259	2D-M624	0.1091	1.0	35	1.0	f ₂	d ₁₄ , ₀₃₄
260	2D-M290	0.1086	1.1	97	90.6	f ₂	θ ₂₃ , ₀₄₅
261	2D-M1	0.106	1.9	309	74.0	f ₂	θ ₁₄ , ₀₂₄
262	2D-M67	0.1059	1.5	264	79.0	f ₂	θ ₁₃ , ₀₁₄
263	2D-M531	0.1058	17.6	605	17.5	f ₂	d ₂₄ , ₀₁₃
264	2D-M463	0.1045	10.5	360	9.5	f ₁	d ₁₃ , ₀₃₅
265	2D-M641	0.1036	1.0	42	1.0	f ₂	d ₂₃ , ₀₂₅
266	2D-M532	0.1028	17.4	597	17.4	f ₂	d ₂₅ , ₀₁₃
267	2D-M636	0.1026	1.0	33	1.0	f ₂	d ₂₄ , ₀₂₅
268	2D-M630	0.1021	1.0	45	1.0	f ₂	d ₁₃ , ₀₂₃
269	2D-M434	0.1012	10.5	361	9.5	f ₁	d ₃₅ , ₀₁₃
270	2D-M29	0.101	8.2	331	7.1	f ₁	d ₁₄ , ₀₄₅
271	2D-M637	0.1006	1.0	5	1.0	f ₂	θ ₂₄ , ₀₃₅
272	2D-M233	0.099	2.5	320	82.4	f ₂	θ ₁₃ , ₀₂₅
273	2D-M77	0.099	1.4	255	63.5	f ₂	θ ₁₃ , ₀₂₄
274	2D-M55	0.0984	1.5	262	78.8	f ₂	θ ₁₄ , ₀₃₄
275	2D-M553	0.097	16.8	575	16.5	f ₂	d ₂₅ , ₀₃₅
276	2D-M42	0.0964	1.4	221	60.2	f ₂	θ ₁₄ , ₀₂₄
277	2D-M642	0.0962	1.0	9	111.0	f ₁	θ ₁₂ , ₀₂₃
278	2D-M255	0.0945	1.8	308	76.7	f ₂	θ ₁₃ , ₀₄₅
279	2D-M409	0.093	10.6	362	9.5	f ₁	d ₃₅ , ₀₁₃
280	2D-M620	0.0923	1.0	16	1.0	f ₂	d ₁₄ , ₀₂₄
281	2D-M452	0.0922	10.6	363	9.5	f ₁	d ₁₃ , ₀₃₅
282	2D-M471	0.091	11.6	403	10.5	f ₁	d ₁₃ , ₀₃₅
283	2D-M179	0.0906	1.0	78	62.8	f ₂	θ ₂₅ , ₀₃₄
284	2D-M438	0.0901	9.2	344	8.1	f ₁	d ₃₅ , ₀₁₃
285	2D-M92	0.0898	1.5	267	62.1	f ₂	θ ₁₃ , ₀₂₃
286	2D-M91	0.0896	1.4	231	49.5	f ₂	θ ₁₃ , ₀₂₃
287	2D-M73	0.088	1.3	197	48.2	f ₂	θ ₁₃ , ₀₄₅
288	2D-M622	0.0869	1.0	39	1.0	f ₂	d ₁₄ , ₀₂₃
289	2D-M365	0.0868	11.6	406	10.5	f ₁	d ₁₄ , ₀₄₅
290	2D-M482	0.0862	1.0	44	1.0	f ₁	d ₁₃ , ₀₃₅
291	2D-M547	0.0855	10.4	357	9.3	f ₂	d ₁₃ , ₀₂₅
292	2D-M426	0.0843	10.6	366	9.5	f ₁	d ₃₅ , ₀₁₃
293	2D-M27	0.0834	11.6	408	10.5	f ₁	d ₁₄ , ₀₄₅
294	2D-M538	0.0833	11.8	416	10.1	f ₁	d ₃₅ , ₀₁₃
295	2D-M495	0.0823	11.6	409	10.5	f ₁	d ₁₃ , ₀₃₅
296	2D-M536	0.0805	19.8	622	19.8	f ₂	d ₄₅ , ₀₁₃
297	2D-M373	0.0742	11.7	412	10.5	f ₁	d ₁₄ , ₀₄₅
298	2D-M280	0.0736	11.7	413	10.5	f ₁	d ₁₃ , ₀₃₅
299	2D-M476	0.073	11.7	414	10.5	f ₁	d ₁₃ , ₀₃₅
300	2D-M377	0.0705	10.8	369	9.5	f ₁	d ₁₄ , ₀₄₅
301	2D-M253	0.0693	11.8	415	10.5	f ₁	d ₃₅ , ₀₁₃
302	2D-M540	0.0692	20.2	629	20.2	f ₂	d ₁₃ , ₀₂₅
303	2D-M539	0.067	20.2	630	20.2	f ₂	d ₁₃ , ₀₂₄
304	2D-M549	0.0656	20.2	626	20.2	f ₂	d ₃₅ , ₀₂₄
305	2D-M552	0.0605	20.2	627	20.2	f ₂	d ₃₅ , ₀₂₅
306	2D-M537	0.0603	20.2	628	20.2	f ₂	d ₄₅ , ₀₁₃
307	2D-M533	0.0579	9.0	336	6.4	f ₁	d ₃₅ , ₀₁₃
308	2D-M32	0.0565	1.0	22	1.0	f ₁	d ₁₄ , ₀₄₅
309	2D-M633	0.0525	1.0	46	1.0	f ₂	d ₁₃ , ₀₄₅
310	2D-M219	0.0514	8.8	333	7.1	f ₁	d ₃₅ , ₀₁₃
311	2D-M422	0.0484	10.1	350	8.4	f ₁	d ₃₅ , ₀₁₃
312	2D-M492	0.0458	1.0	10	1	f ₁	d ₁₃ , ₀₃₅
313	2D-M379	0.0441	12.2	433	10.5	f ₁	d ₁₄ , ₀₄₅
314	2D-M487	0.0401	12.3	436	10.5	f ₁	d ₁₃ , ₀₃₅
315	2D-M420	0.0335	14.1	512	14.2	f ₂	d ₂₃ , ₀₁₃
316	2D-M589	0.0333	1.0	37	1.0	f ₁	d ₁₃ , ₀₃₅
317	2D-M613	0.0326	1.0	47	1.0	f ₁	d ₁₃ , ₀₃₅
318	2D-M498	0.032	17.2	580	17.4	f ₂	d ₂₄ , ₀₂₅
319	2D-M352	0.0318	17.3	585	17.3	f ₂	d ₁₄ , ₀₃₅
320	2D-M157	0.0297	20.8	636	20.1	f ₂	d ₁₄ , ₀₂₄
321	2D-M262	0.0296	11.2	388	18.1	f ₂	d ₁₃ , ₀₂₃
322	2D-M218	0.0294	17.0	579	16.8	f ₂	d ₄₅ , ₀₁₃
323	2D-M542	0.0293	16.8	573	15.8	f ₂	d ₁₃ , ₀₂₃
324	2D-M172	0.0289	17.5	601	15.1	f ₂	d ₁₄ , ₀₂₃
325	2D-M205	0.028	14.6	535	18.9	f ₂	d ₁₄ , ₀₁₃
326	2D-M394	0.0271	12.8	451	8.6	f ₂	d ₂₃ , ₀₃₄
327	2D-M520	0.027	19.4	618	18.1	f ₂	d ₁₄ , ₀₂₅
328	2D-M421	0.0268	17.3	586	17.3	f ₂	d ₄₅ , ₀₁₃
329	2D-M360	0.0268	17.3	582	17.3	f ₂	d ₁₄ , ₀₂₃
330	2D-M413	0.0267	13.2	472	12.9	f ₂	d ₄₅ , ₀₁₃
331	2D-M355	0.0266	14.1	523	14.1	f ₂	d ₁₄ , ₀₃₅
332	2D-M349	0.0263	14.6	536	14.5	f ₂	d ₁₄ , ₀₂₄
333	2D-M508	0.0263	17.6	606	16.4	f ₂	d ₂₅ , ₀₂₄
334	2D-M407	0.0261	14.9	541	14.9	f ₂	d ₁₄ , ₀₁₃
335	2D-M389	0.026	17.4	594	6.4	f ₂	d ₁₄ , ₀₃₄
336	2D-M424	0.0259	16.1	561	18.4	f ₂	d ₂₅ , ₀₁₃
337	2D-M450	0.0258	13.1	460	13.0	f ₂	d ₁₃ , ₀₂₄
338	2D-M534	0.0254	19.9	624	18.6	f ₂	d ₂₃ , ₀₁₃
339	2D-M548	0.0253	19.0	615	17.8	f ₂	d ₂₅ , ₀₂₄
340	2D-M387	0.0245	17.3	590	6.4	f ₂	d ₁₄ , ₀₂₃
341	2D-M412	0.0244	13.1	463	13.1	f ₂	d ₁₄ , ₀₁₃
342	2D-M543	0.0241	18.5	610	18.0	f ₂	d ₁₃ , ₀₂₅
343	2D-M556	0.024	20.4	633	18.6	f ₂	d ₂₅ , ₀₂₃
344	2D-M346	0.0239	14.8	538	12.3	f ₂	d ₁₄ , ₀₂₄
345	2D-M475	0.0238	17.0	578	17.5	f ₂	d ₁₃ , ₀₂₅
346	2D-M288	0.0238	15.0	543	14.8	f ₂	d ₃₅ , ₀₂₃
							...continued

continuing...							
S.No.	Name	μ	κ	i_{κ}	μ	f	AJV
347	2D-M507	0.0235	17.3	588	17.3	f ₂	d ₃₅ , ₀₂₄
348	2D-M348	0.0235	17.3	587	17.3	f ₂	d ₁₄ , ₀₂₄
349	2D-M163	0.0234	13.7	481	12.6	f ₂	d ₁₄ , ₀₂₃
350	2D-M242	0.023	18.4	609	13.8	f ₂	d ₄₅ , ₀₁₃
351	2D-M550	0.023	19.1	617	17.7	f ₂	d ₂₄ , ₀₃₅
352	2D-M24	0.0228	14.5	532	12.1	f ₂	d ₁₄ , ₀₂₄
353	2D-M425	0.0226	14.1	522	14.1	f ₂	d ₄₅ , ₀₁₃
354	2D-M357	0.0223	17.4	595	16.9	f ₂	d ₁₄ , ₀₂₃
355	2D-M535	0.0222	19.8	623	18.4	f ₂	d ₂₅ , ₀₁₃
356	2D-M406	0.0222	13.9	494	15.1	f ₂	d ₁₄ , ₀₁₃
357	2D-M156	0.0222	16.8	572	13.6	f ₂	d ₁₄ , ₀₂₄
358	2D-M252	0.0219	20.3	632	14.3	f ₂	d ₄₅ , ₀₁₃
359	2D-M628	0.0217	1.0	26	1.0	f ₂	d ₁₃ , ₀₂₅
360	2D-M366	0.0215	13.0	458	12.9	f ₂	d ₁₄ , ₀₃₄
361	2D-M343	0.0215	12.1	429	7.8	f ₂	d ₂₅ , ₀₁₄
362	2D-M155	0.0215	16.3	563	13.9	f ₂	d ₁₄ , ₀₂₄
363	2D-M194	0.0214	16.3	562	13.6	f ₂	d ₁₄ , ₀₁₃
364	2D-M502	0.0214	17.3	584	17.3	f ₂	d ₃₅ , ₀₂₃
365	2D-M374	0.0214	17.3	583	17.3	f ₂	d ₁₄ , ₀₂₅
366	2D-M192	0.0213	16.1	560	13.2	f ₂	d ₁₄ , ₀₁₃
367	2D-M354	0.021	17.0	577	14.6	f ₂	d ₁₄ , ₀₂₅
368	2D-M168	0.0209	14.0	498	12.5	f ₂	d ₁₄ , ₀₂₅
369	2D-M353	0.0208	14.3	531	11.8	f ₂	d ₁₄ , ₀₃₅
370	2D-M465	0.0205	14.0	506	14.0	f ₂	d ₁₃

continuing...							
S.No.	Name	μ	κ	$i\kappa$	μ	f	AJV
454	2D-M279	0.0144	12.5	440	8.7	f_2	d_{13}, θ_{45}
455	2D-M417	0.0143	13.1	465	11.3	f_2	d_{24}, θ_{13}
456	2D-M386	0.0143	17.3	589	5.3	f_2	d_{14}, θ_{23}
457	2D-M342	0.0142	17.4	593	5.2	f_2	d_{23}, θ_{14}
458	2D-M488	0.0141	13.1	461	11.3	f_2	d_{13}, θ_{25}
459	2D-M167	0.014	10.6	365	7.0	f_2	d_{14}, θ_{24}
460	2D-M501	0.0139	14.0	501	10.6	f_2	d_{45}, θ_{23}
461	2D-M368	0.0139	14.0	502	10.6	f_2	d_{14}, θ_{25}
462	2D-M480	0.0139	16.4	566	10.3	f_2	d_{13}, θ_{23}
463	2D-M258	0.0139	9.8	346	6.8	f_2	d_{13}, θ_{24}
464	2D-M392	0.0139	18.5	612	4.9	f_2	d_{25}, θ_{23}
465	2D-M189	0.0139	13.8	491	10.4	f_2	d_{45}, θ_{13}
466	2D-M154	0.0138	13.6	479	10.3	f_2	d_{14}, θ_{24}
467	2D-M261	0.0138	14.0	507	10.6	f_2	d_{13}, θ_{23}
468	2D-M510	0.0138	9.9	347	7.1	f_2	d_{23}, θ_{25}
469	2D-M399	0.0138	16.6	568	11.0	f_2	d_{14}, θ_{13}
470	2D-M14	0.0138	10.8	371	6.9	f_2	d_{14}, θ_{24}
471	2D-M324	0.0137	13.8	488	10.6	f_2	d_{24}, θ_{14}
472	2D-M382	0.0137	19.9	625	5.8	f_2	d_{14}, θ_{25}
473	2D-M271	0.0136	13.9	496	10.5	f_2	d_{13}, θ_{24}
474	2D-M403	0.0136	11.1	380	7.1	f_2	d_{14}, θ_{13}
475	2D-M333	0.0136	13.9	497	10.5	f_2	d_{25}, θ_{14}
476	2D-M12	0.0136	12.2	434	8.9	f_2	d_{14}, θ_{24}
477	2D-M356	0.0136	10.8	372	7.2	f_2	d_{14}, θ_{23}
478	2D-M331	0.0132	13.1	459	9.5	f_2	d_{23}, θ_{14}
479	2D-M269	0.0132	13.5	476	10.8	f_2	d_{13}, θ_{25}
480	2D-M281	0.0132	10.0	349	7.0	f_2	d_{13}, θ_{25}
481	2D-M351	0.0132	14.2	528	10.8	f_2	d_{14}, θ_{25}
482	2D-M431	0.0132	14.2	527	10.8	f_2	d_{23}, θ_{13}
483	2D-M337	0.0132	12.0	424	8.4	f_2	d_{34}, θ_{14}
484	2D-M166	0.0132	14.0	499	9.4	f_2	d_{14}, θ_{25}
485	2D-M265	0.0131	14.0	500	10.5	f_2	d_{13}, θ_{25}
486	2D-M393	0.0131	18.5	611	4.9	f_2	d_{23}, θ_{25}
487	2D-M462	0.0131	14.0	503	10.5	f_2	d_{13}, θ_{45}
488	2D-M436	0.0131	14.0	504	10.5	f_2	d_{25}, θ_{13}
489	2D-M334	0.0131	14.0	505	10.5	f_2	d_{34}, θ_{14}
490	2D-M329	0.013	12.0	425	8.4	f_2	d_{23}, θ_{14}
491	2D-M384	0.013	21.4	639	10.5	f_2	d_{14}, θ_{25}
492	2D-M395	0.013	21.3	638	10.5	f_2	d_{25}, θ_{23}
493	2D-M396	0.013	19.7	619	7.1	f_2	d_{23}, θ_{25}
494	2D-M162	0.013	10.8	368	7.1	f_2	d_{14}, θ_{23}
495	2D-M206	0.013	10.9	374	8.2	f_2	d_{14}, θ_{13}
496	2D-M274	0.013	12.0	423	8.5	f_2	d_{13}, θ_{23}
497	2D-M511	0.013	13.9	495	10.6	f_2	d_{23}, θ_{25}
498	2D-M418	0.0129	14.0	508	10.5	f_2	d_{25}, θ_{13}
499	2D-M350	0.0129	14.1	510	10.5	f_2	d_{14}, θ_{25}
500	2D-M370	0.0129	13.1	464	9.5	f_2	d_{14}, θ_{24}
501	2D-M339	0.0129	11.3	394	7.1	f_2	d_{23}, θ_{14}
502	2D-M347	0.0129	14.0	509	10.5	f_2	d_{14}, θ_{24}
503	2D-M479	0.0129	13.8	492	10.3	f_2	d_{13}, θ_{23}
504	2D-M287	0.0129	14.3	529	8.8	f_2	d_{45}, θ_{23}
505	2D-M19	0.0129	10.8	373	7.1	f_2	d_{14}, θ_{45}
506	2D-M470	0.0128	13.1	466	9.5	f_2	d_{13}, θ_{45}
507	2D-M506	0.0128	11.8	418	8.1	f_2	d_{45}, θ_{24}
508	2D-M437	0.0128	12.1	426	8.4	f_2	d_{45}, θ_{13}
509	2D-M401	0.0128	13.1	468	9.5	f_2	d_{14}, θ_{13}
510	2D-M338	0.0128	17.3	581	9.5	f_2	d_{23}, θ_{14}
511	2D-M464	0.0127	14.1	513	10.5	f_2	d_{13}, θ_{25}
512	2D-M433	0.0127	13.1	469	9.5	f_2	d_{45}, θ_{13}
513	2D-M423	0.0127	13.8	490	10.2	f_2	d_{25}, θ_{13}
514	2D-M472	0.0127	13.1	462	9.6	f_2	d_{13}, θ_{25}
515	2D-M336	0.0127	14.1	515	10.5	f_2	d_{25}, θ_{14}
516	2D-M321	0.0126	12.1	427	8.4	f_2	d_{24}, θ_{14}
517	2D-M380	0.0126	15.7	557	10.2	f_2	d_{14}, θ_{23}
518	2D-M335	0.0126	14.1	516	10.5	f_2	d_{25}, θ_{14}
519	2D-M21	0.0126	12.1	428	8.4	f_2	d_{24}, θ_{14}
520	2D-M345	0.0126	13.2	470	9.5	f_2	d_{14}, θ_{24}
521	2D-M367	0.0126	14.1	517	10.5	f_2	d_{14}, θ_{45}
522	2D-M25	0.0126	13.2	471	9.5	f_2	d_{14}, θ_{25}
523	2D-M320	0.0126	14.1	518	10.5	f_2	d_{24}, θ_{14}
524	2D-M30	0.0125	14.1	519	10.5	f_2	d_{14}, θ_{13}
525	2D-M323	0.0125	12.7	447	7.5	f_2	d_{24}, θ_{14}
526	2D-M428	0.0123	16.8	576	10.1	f_2	d_{24}, θ_{13}
527	2D-M496	0.0121	14.1	521	9.9	f_2	d_{13}, θ_{25}
528	2D-M455	0.0121	12.6	443	8.1	f_2	d_{13}, θ_{23}
529	2D-M330	0.0121	13.7	483	9.2	f_2	d_{23}, θ_{14}
530	2D-M449	0.0121	9.0	338	5.1	f_2	d_{13}, θ_{24}
531	2D-M169	0.012	10.6	364	8.1	f_2	d_{14}, θ_{25}
532	2D-M161	0.012	15.3	550	10.1	f_2	d_{14}, θ_{23}
533	2D-M402	0.0119	13.7	486	8.8	f_2	d_{14}, θ_{13}
534	2D-M446	0.0119	15.6	554	9.5	f_2	d_{13}, θ_{45}
535	2D-M429	0.0119	13.8	493	8.5	f_2	d_{24}, θ_{13}
536	2D-M358	0.0117	13.5	474	9.6	f_2	d_{14}, θ_{23}
537	2D-M275	0.0117	13.7	484	7.0	f_2	d_{13}, θ_{45}
538	2D-M272	0.0117	13.1	467	9.2	f_2	d_{13}, θ_{25}
539	2D-M327	0.0116	14.6	534	9.4	f_2	d_{23}, θ_{14}
540	2D-M322	0.0116	14.6	533	9.5	f_2	d_{24}, θ_{14}
541	2D-M490	0.0115	24.5	642	8.4	f_2	d_{13}, θ_{45}
542	2D-M505	0.0114	24.4	640	8.4	f_2	d_{23}, θ_{45}
543	2D-M13	0.0113	13.5	477	9.3	f_2	d_{14}, θ_{25}
544	2D-M18	0.0112	12.3	437	8.4	f_2	d_{14}, θ_{13}
545	2D-M432	0.0111	15.6	555	7.4	f_2	d_{23}, θ_{13}
546	2D-M341	0.011	17.3	592	2.9	f_2	d_{23}, θ_{14}
547	2D-M400	0.0109	26.1	644	7.8	f_2	d_{14}, θ_{13}
548	2D-M191	0.0108	15.3	552	8.0	f_2	d_{25}, θ_{13}
549	2D-M20	0.0107	8.7	332	6.6	f_2	d_{14}, θ_{25}
550	2D-M388	0.0107	17.3	591	2.9	f_2	d_{14}, θ_{25}
551	2D-M448	0.0105	12.2	432	5.8	f_2	d_{13}, θ_{25}
552	2D-M325	0.0104	16.7	571	8.1	f_2	d_{25}, θ_{14}
553	2D-M270	0.0098	16.7	570	6.6	f_2	d_{13}, θ_{24}
554	2D-M643	0.0091	14.8	539	10.5	f_1	θ_{12}, d_{23}
555	2D-M644	0.0091	14.8	540	10.5	f_1	d_{12}, θ_{23}
556	2D-M416	0.0088	25.6	643	7.1	f_2	d_{24}, θ_{13}
557	2D-M195	0.0085	16.7	569	4.9	f_2	d_{14}, θ_{13}
558	2D-M197	0.0084	13.6	480	4.5	f_2	d_{14}, θ_{13}
559	2D-M22	0.0082	18.9	614	6.1	f_2	d_{25}, θ_{14}
560	2D-M326	0.0079	16.4	564	5.8	f_2	d_{23}, θ_{14}

...continued

continuing...							
S.No.	Name	μ	κ	$i\kappa$	μ	f	AJV
561	2D-M486	0.0079	16.4	565	5.8	f_2	d_{13}, θ_{45}
562	2D-M398	0.0078	27.4	645	6.4	f_2	d_{14}, θ_{13}
563	2D-M171	0.0077	16.1	559	4.5	f_2	d_{14}, θ_{23}
564	2D-M391	0.0073	20.2	631	3.4	f_2	d_{14}, θ_{34}
565	2D-M332	0.0066	19.0	616	5.5	f_2	d_{25}, θ_{14}
566	2D-M494	0.0062	21.2	637	5.1	f_2	d_{13}, θ_{45}
567	2D-M509	0.0057	19.7	620	4.8	f_2	d_{23}, θ_{45}
568	2D-M328	0.0055	17.5	600	3.5	f_2	d_{23}, θ_{14}
569	2D-M176	0.0041	16.8	574	2.7	f_2	d_{14}, θ_{25}
570	2D-M599	0.0028	1.0	53	1.0	f_2	d_{13}, θ_{25}
571	2D-M40	0.0026	1.7	304	1.7	f_2	d_{13}, d_{45}
572	2D-M469	0.0021	1.1	106	1.1	f_2	d_{13}, d_{25}
573	2D-M483	0.002	1.1	79	1.0	f_2	d_{13}, d_{25}
574	2D-M565	0.002	1.0	50	1.0	f_2	d_{14}, d_{25}
575	2D-M36	0.002	1.4	238	1.4	f_2	d_{14}, d_{24}
576	2D-M560	0.0019	1.2	147	1.2	f_2	d_{14}, d_{24}
577	2D-M573	0.0018	1.2	146	1.2	f_2	d_{14}, d_{25}
578	2D-M441	0.0017	1.1	124	1.1	f_2	d_{13}, d_{14}
579	2D-M39	0.0017	1.2	165	1.2	f_2	d_{13}, d_{14}
580	2D-M563	0.0017	1.1	94	1.1	f_2	d_{14}, d_{24}
581	2D-M576	0.0017	1.1	85	1.1	f_2	d_{14}, d_{25}
582	2D-M575	0.0017	1.1	87	1.1	f_2	d_{14}, d_{25}
583	2D-M587	0.0017	1.1	91	1.1	f_2	d_{13}, d_{14}
584	2D-M615	0.0016	1.0	71	1.0	f_2	d_{24}, d_{25}
585	2D-M588	0.0016	1.1	86	1.1	f_2	d_{13}, d_{45}
586	2D-M34	0.0016	1.5	261	1.0	f_2	d_{13}, d_{14}
587	2D-M493	0.0016	1.1	90	1.1	f_2	d_{13}, d_{25}
588	2D-M574	0.0016	1.0	12	1.0	f_2	d_{14}, d_{34}
589	2D-M467	0.0016	1.1	126	1.1	f_2	<